CHALMERS

Evaluation of driver models for left turn across path manoeuvres

Master's Thesis in Automotive Engineering

PATRICK BARDINET DE HORNA

FRANCESCO SECONDO

Department of Applied Mechanics
Division of Vehicle Safety
CHALMERS UNIVERSITY OF TECHNOLOGY
Göteborg, Sweden 2014
Master's thesis 2014:53

MASTER'S THESIS IN AUTOMOTIVE ENGINEERING

Evaluation of driver models for left turn across path manoeuvres

PATRICK BARDINET DE HORNA

FRANCESCO SECONDO

Department of Applied Mechanics
Division of Vehicle Safety
CHALMERS UNIVERSITY OF TECHNOLOGY

Göteborg, Sweden 2014

Evaluation of driver models for left turn across path manoeuvres

PATRICK BARDINET DE HORNA
FRANCESCO SECONDO

Master's Thesis 2014:53
ISSN 1652-8557
Department of Applied Mechanics
Division of Vehicle Safety
Chalmers University of Technology
SE-412 96 Göteborg
Sweden
Telephone: + 46 (0)31-772 1000

Chalmers Reproservice
Göteborg, Sweden 2014

Evaluation of driver models for left turn across path manoeuvres
Master's Thesis in *Master's Thesis in Automotive Engineering*
PATRICK BARDINET DE HORNA
FRANCESCO SECONDO
Department of Applied Mechanics
Division of Vehicle Safety
Chalmers University of Technology

ABSTRACT

Accidents at intersections are one of the most common causes of fatalities on roads. Statistics from the EU and the USA show that fatalities at intersections represent more than one fifth of all traffic fatalities. In particular, the left turn across the path of a vehicle coming from the opposite direction (LTAP/OD) is one of the riskiest situations at intersections. The goal of the thesis is to develop driver models describing human behaviour during left-turn-across path scenarios, for future use in active safety systems development for intersections. Video and vehicle dynamics data during daily driving were retrieved from the EuroFOT project database in order to find LTAP/OD scenarios suitable for the scope of the thesis. For the description of driver's behaviour during the LTAP/OD scenario, two different driver modelling approaches have been considered: the Salvucci and Gray's, which focuses on steering behaviour, and Nobukawa's, which is based on vehicle acceleration. The work has been performed using MATLAB®, exploiting also genetic algorithms for model parameter optimization. The models describe the steering and speed behaviour reasonably well for the specific LTAP/OD events used in the model optimization and validation. However, generalization cannot be made across LTAP/OD as a scenario. Further efforts are required, e.g., to increase of number of intersections and number of drivers in the validation, to verify the reliability of the two models and develop it further. Once reliability has been established, the models may be used as part of the design of Intersection Driver Support Systems.

Keywords: Driver behaviour, Driver models, Human Factors, Intersection, Naturalistic data, Post Encroachment Time, Road Safety.

PREFACE

This thesis work has been carried out in order to complete the Master of Science degree in Automotive Engineering at Chalmers University of Technology in Goteborg, Sweden. All the stages of the project were performed at SAFER, Vehicle and Traffic Safety Centre at Chalmers University of Technology during January-June 2014. Data to analyse were retrieved from naturalistic studies performed, with the support of Volvo Cars, as part of the EuroFOT project, whose final event was on 26th – 27th June 2012 in Brussels.

We would like to acknowledge and thank our examiner Jonas Bärgman and our supervisor Giulio Piccinini for the opportunity they offered to us to be involved into this amazing and challenging project and for their constant guidance and support along the development of our work.
We would also like to thank Ola Benderius, always available to give to us precious suggestions when the faced situation was hard to solve.
Last, but not least, we would like to remember all the people we met in SAFER during this semester (Erik, Lisa, Christian-Nils, Leyla, Martin and many others); everybody has always been very kind with us and was able to make us feel like at home. We are proud to be part of this "family" and we will never forget you.

Patrick Bardinet de Horna would like to acknowledge his family and friends. First of all, to my parents, brother and sister that always supported me no matter what and gave me the opportunity to study in Sweden and made this experience possible. Your eternal support, encouragement and love during this period of my life made it unforgettable. To all my friends from all around the world that made these years the best experience I could have ever imagined. To all of them thank you.

Francesco Secondo would also like to acknowledge his family and friends. My parents always supported me with unbelievable patience and they always pushed me in doing my best, giving to me the opportunity to study in Sweden for the entire academic year. Tack så mycket to all my friends from all around the world I met during these five years of university career. Hope to see all of them soon again.

Table of Contents

1 Introduction

1.1 Background

Car crashes often occur at intersections because these locations, where two or more roads cross each other, lead to the management of complex manoeuvres. Examples of such manoeuvres are turning left, crossing over, and turning right, and have the potential for causing accidents. The American Fatality Analysis Reporting System (FARS) and the National Automotive Sampling System-General Estimates System (NASS-GES) data show that about 40 percent of the estimated 5,811,000 crashes that occurred in the United States in 2008 were intersection-related crashes (National Highway Traffic Safety Administration, 2010). Characteristics of intersection-related crashes (traffic control devices, critical pre-crash event, and atmospheric conditions) as well as of the drivers (age, sex, and driving behaviour) can provide useful guidelines for crash prevention. This brief introduction only considers the main assigned critical reasons related to specific scenarios.
In the National Motor Vehicle Crash Causation Survey (NMVCCS), the variable "critical pre-crash event" is defined as an event that made the crash imminent or inevitable (National Highway Traffic Safety Administration, 2008). It is coded for each vehicle in the crash and documents the circumstances leading to this vehicle's first impact in the crash sequence. Figure 1.1 shows the distribution of crashes over critical pre-crash events. Out of an estimated 2,188,969 NMVCCS crashes, about 36% (787,236) are critical pre-crash events related to turning or crossing at intersections. In 22.2% of these intersection-related crashes, the critical event was turning left, while passing straight through the intersection (crossing-over) constituted 12.6% of such critical pre-crash events and turning right at the intersection accounted for a very small percentage (1.2%) of vehicles. Due to the multiple choice nature of this variable and of the following ones, the percentages in some of the figures and the total sum in some of the tables may not be completely in line.

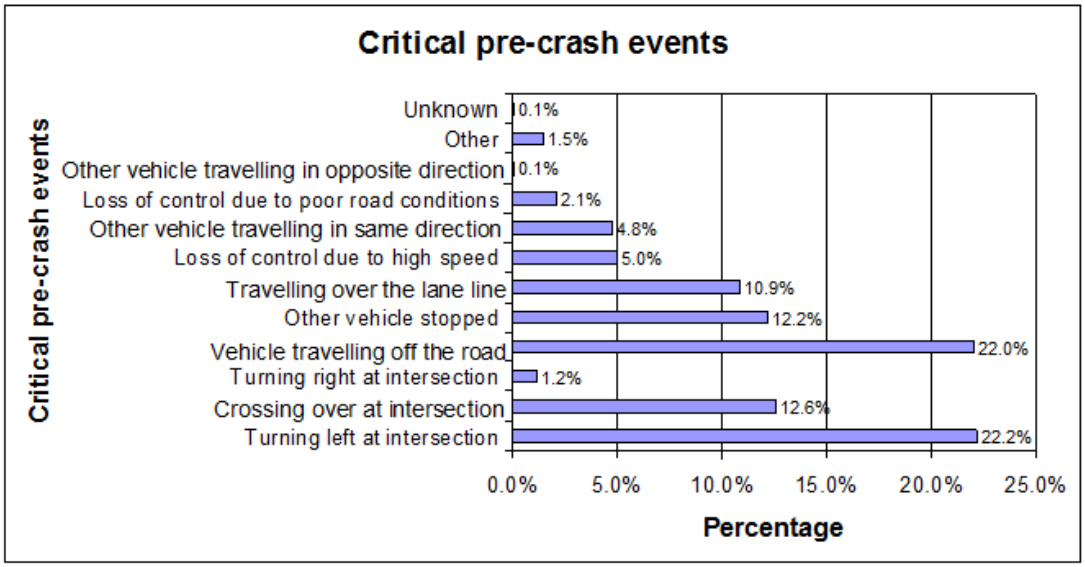

Figure 1.1: Distribution of critical pre-crash events

In the NMVCCS, the variable "traffic control device" includes all traffic control devices that regulate vehicular traffic on the roadway on which a vehicle is travelling just prior to a critical pre-crash event. This excludes devices that solely regulate pedestrians, such as walk signals. Note that the coding of this variable is based on multiple choices per vehicle. Intersections in this sample (from the US) are often controlled by traffic signals or stop signs but some have neither. Figure 1.2 shows the distribution of intersection-related crashes per traffic control device. In an estimated 787,236 intersection-related crashes, 52.5% (413,140) of the vehicles were travelling on roadways that were controlled by at least one traffic signal and 31.3% (246,385) by at least one stop sign. About 15.9% (125,022) of vehicles were travelling on the roadways with no traffic control device.

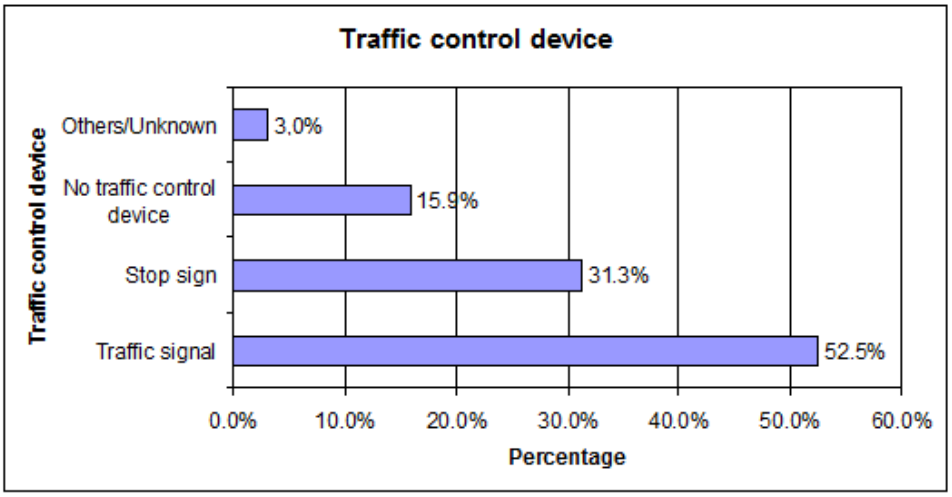

Figure 1.2: Distribution of traffic control devices

In more recent years, statistics from the EU and the USA show that fatalities at junctions represent more than 20% of all traffic fatalities. In the European Union, fatalities at intersections have remained relatively constant between 2000 and 2009, where this percentage has only fluctuated between 20% and 22% (ERSO, 2008). These numbers are comparable to the USA, where in 2011, as shown in Table 1.1 (National Highway Traffic Safety Administration, 2011), 9525 fatalities over 43945 (that is, 21.63%) happened at intersections. In 2010, the percentage of fatalities at intersection was 22.31%.

Table 1.1: Vehicles involved by relation to junction and traffic control device

Relation to junction	Traffic Control Device				
	None	Traffic signal	Stop sign	Other/Unknown	Total
Non-Junction	26495	58	16	1812	28381
Junction – Intersection	3772	3389	2078	286	9525
Junction – Intersection related	1143	880	260	118	2401
Other/Unknown	3108	97	79	354	3638
Total	34518	4424	2433	2570	43945

The causes of accidents at junctions are numerous, but research suggest that in Europe around 60% of the incidents are related to an inappropriate timing from the driver (e.g. premature, late, or no action) (ERSO, 2008). Inappropriate timing could be linked to several causes and the most common ones are faulty diagnosis, information failure, observation missed and inadequate plan.
This study is focused on the left turn situations or, more specifically, the left-turn-across-path opposite-direction (LTAP/OD) manoeuvres, since this scenario is likely to have more encroachments than other events and since the crashes for this situation represent a big part of the intersection-related crashes (Chan, 2005); thus, it turns out to be one of the riskiest situations at intersections (Preusser et al., 1998). The car which turns is hereafter called the Subject Vehicle (SV) while the vehicle that is oncoming (going straight or turning left or right) is called the Principal Other Vehicle (POV), as shown in Figure 1.3. That is, we focus our analysis in this thesis on the left turning vehicle and its driver.

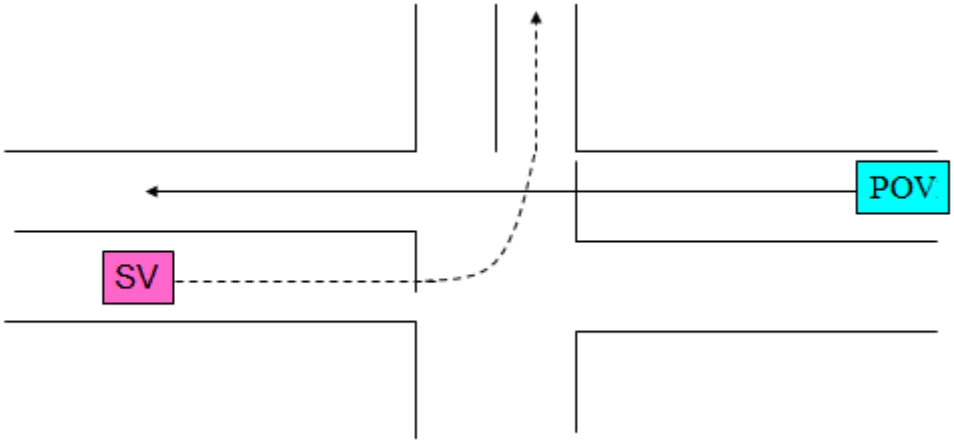

Figure 1.3: LTAP/OD scenario

1.2 Advanced Driver Assistance Systems (ADAS)

The best way to avoid crashes is to prevent the occurrence of a hazardous situation. When approaching an intersection, the SV driver must judge whether it is safe to cross the opposing traffic lane at both signalized and unsignalized intersections. If the intersection is signalized, the SV driver must also consider the signal status. If the SV has no possibility to complete the turning manoeuvre when opposing traffic is oncoming, a warning can be issued to the SV driver (for example, warnings to stop, to brake or to not steer) when a hazard exists.
In recent years, the implementation of ADAS is having an increasing trend. The main reason of that is safety but also comfort to the driver together with environmental aspects play an important role (Brookhuis et al., 2001). In Europe, USA and Japan, combined ergonomic and engineering approaches to both hazard assessment and the indication of drivers' performance limits have developed into research and implementation of new ADAS to improve driving safety and comfort (Brookhuis et al., 1992). Well-known examples of this type of applications are navigation or route guidance systems and adaptive cruise control systems. Though expensive, prototypes of such systems passed a number of tests (and improvements) and were successfully placed on the consumer market. Marketing research has been indispensable to understand customer needs, but also studies on devices acceptance and certain safety

effects are still required after implementation. Finally, environmental issues are not decisive in this area yet, but it is forecast it will gain weight in the future.
ADAS concepts include blind spot detectors (Congress, 1994), Adaptive Cruise Control (Rosengren, 1995), Forward Collision Warning Systems (Rumar, 1988), Automatic Emergency Braking (Verwey et al., 1996) and Intersection Decision Support Systems (IDSS) (Bekiaris et al.,1997). Some of these technologies are available on the market, or ready to be marketed, while others are still in a developing stage or ready to be evaluated as prototypes.

1.2.1 Benefits and drawbacks of ADAS

The main purpose of ADAS is that driver error consequences will be reduced or even eliminated, because the system will support the driver in getting attention back, and overall vehicle performance is enhanced. The benefits of ADAS implementations are potentially great because of a significant decrease in human mental and physical suffering, in economical cost and in pollution, since:

- driving safety would be considerably enhanced, as human errors, which are responsible or concurrent for about 95% of overall accidents (Treat et al., 1979), would be identified and their consequences would be prevented, or at least mitigated;
- high-performance driving can be conducted without regard to visual obstacles, weather and environmental conditions;
- drivers using ADAS can be safe and efficient drivers.

Primary functionality of ADAS is to facilitate the task performance of drivers by providing real-time advice, instruction, warnings and event interventions (e.g. braking). ADAS may operate in advisory, semi-automatic or automatic mode, all of which may have different consequences for the driving task, and with that on traffic safety.
Although the purpose of an ADAS is to have a positive effect on traffic safety, it has been shown they can also have some unwanted secondary negative effects (Brookhuis et al., 2001). Firstly, such a great amount of information potentially leads to a situation where the driver's attention is diverted from traffic. Secondly, drivers' negative behavioural adaptation to such systems could prevent the driver to be aware in time of a sudden hazard, or to be ready for an adequate reaction. Thirdly, the driver could over-trust the ADAS. Before introducing any ADAS, the consequences of system implementation in this sense should be identified.
A specific source of problems with the development of ADAS that are intended to reduce accidents is that it is very difficult to forecast the savings in terms of fatalities and injuries that might result from the introduction of such systems. Although there is an urgent need to know what the effects of a specific system are before it enters the market, no actual data about system benefits and risks exist until it is operative on real-world environment. One type of effects which can be studied before marketing are those related to the behavioural aspects of the driving task, in order to pinpoint both beneficial and unwanted side effects at the driver level.

1.2.2 Acceptance/attitude towards ADAS

A basic question in ADAS implementations is whether it will be accepted or not, i.e. giving up parts of the direct control over the vehicle or receive warnings (Brookhuis et al., 2001). It is important to understand which are the decisions or the situations which the driver prefers to be handled by the vehicle. In some cases, although drivers expect a positive safety effect by ADAS, they have at the same time reservations against them. Handing over control to a device and the automated braking function, for instance, are evaluated as negative aspects of ADAS systems for some people. An international questionnaire survey has been carried out during the SAVE project (EU DG XIII TR1047, 1999) and it has indicated that the driver population is reluctant to totally release vehicle control, but is willing to accept it in emergency situations. Another obstacle to ADAS acceptance is given by system supervision and adjustments from the human operator: normal operations are, indeed, performed automatically, while if something goes wrong with the system, unusual actions are required to the driver (Bainbridge, 1983). Such situations are rare, but also dangerous, and driver experience in this field is very limited; moreover, human problem solving is not optimal if the situation requires a quick reaction.
All in all, the potential of ADAS is great, provided ADAS will be accepted and widely introduced. Acceptance of ADAS is highly dependent upon solid demonstration of the systems themselves are reliable in both ordinary and critical situations. For the end-user the benefits should be clear and preferably directly noticeable; false alarms are not acceptable for end-users particularly.

1.2.3 Criteria in Intersection Decision Support Systems

In intersection situations, as well as in most of road safety scenarios, the driver behaviour and the vehicle dynamics should be taken into account. Intersection Decision Support Systems (IDSS) is meant to provide a driver the information needed to make correct decisions regarding the available gap while dealing with an intersection. The system is designed to provide the safety benefits of a signalized intersection (fewer crashes, opportunities for all drivers to enter/cross the traffic stream), while minimizing the drawbacks (installation expenses, disruption of traffic flow). IDSS, however, do not provide additional opportunities for drivers to enter/cross the traffic stream, since it doesn't create gaps that were not present. When developing an IDSS, it is necessary to identify and quantify in what situations drivers would accept its interventions. In general, for many ADAS, it is necessary to define some setting parameters, called safety thresholds (Cody, 2011), in order to evaluate if the system timely warns the driver or intervenes, without creating false interventions/alarms or late warnings; safety thresholds can differ from one IDSS design to another and must suit to the different driving behaviours. These safety thresholds are measured in terms of gap between vehicles and can be expressed as a distance or as a time. As an example (Figure 1.4), the safety threshold chosen for the IDS design can be the temporal gap between two vehicles on the major-road to determine when it is safe for an opponent car to turn at the intersection (Laberge et al., 2006 and Ragland et al., 2006). Another safety threshold can be the trailing buffer (Chan, 2006), which corresponds to the time measured from the moment when the SV passes the point of conflict to the moment when the POV (Principal Other Vehicle) reaches the same point. Finally, the PET (Post-Encroachment Time) criterion is commonly used to characterize a posteriori how risky the encroachment was. PET is

however a post-hoc measure, defined as the time measured from the moment in which the SV leaves the encroachment zone (Figure 1.5 - t1) to the moment in which the POV enters this zone (Figure 1.5 - t2) (Allen, al.,1978).

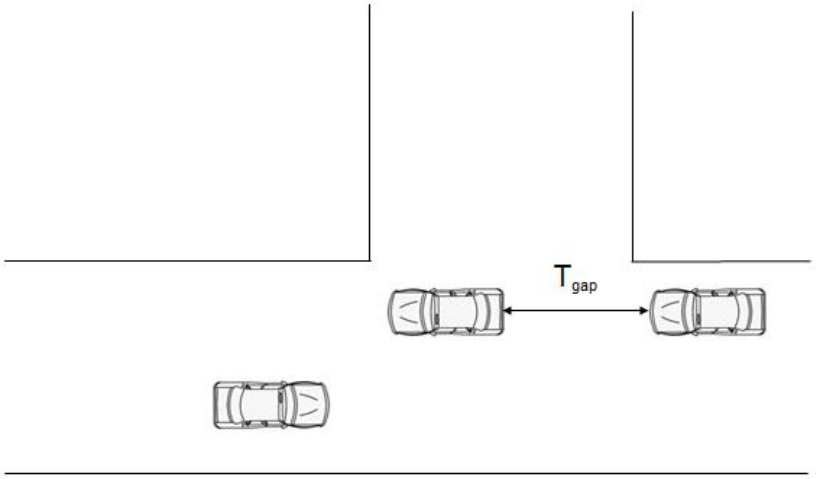

Figure 1.4: Temporal gap definition

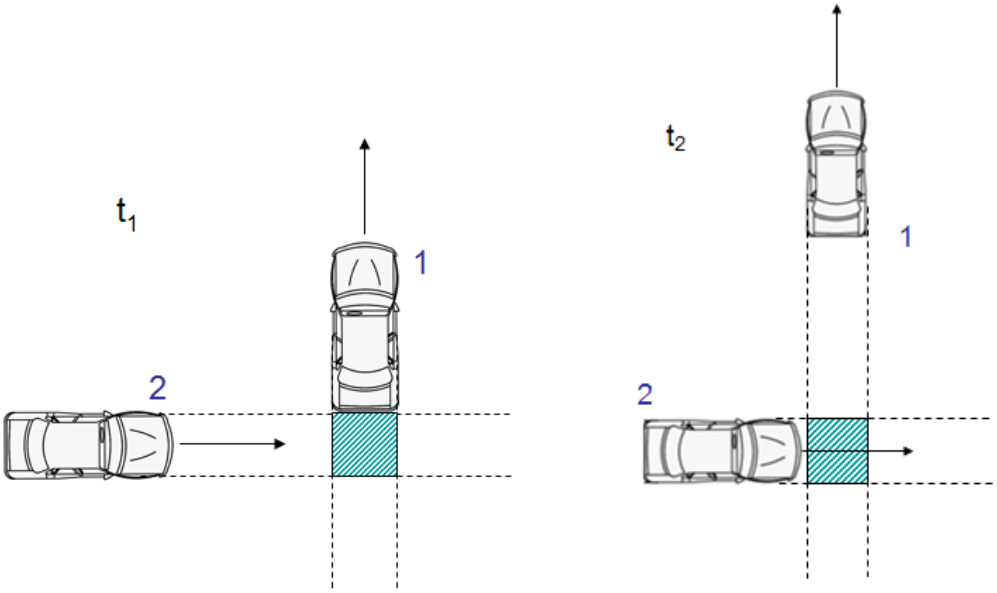

Figure 1.5: Post Encroachment Time definition; PET = t_2-t_1

1.3 Naturalistic driving data

Naturalistic driving data collected during real crashes and near-crashes situations constitute a reliable method to evaluate the performance of IDSS before marketing them. Data describing vehicle speeds, ranges, driver decelerations, and even driver reaction time have been estimated and used as inputs into models to guide alert design or to predict IDSS benefits.

Naturalistic driving data are information collected from a large number of drivers and vehicles over an extended period of time. Data are classified by pre-event manoeuvre, precipitating factor, event type, contributing factors and the avoidance manoeuvre.

The first large study conducted in this particular field was the 100-Car Naturalistic Driving Study, where 100 ordinary cars were equipped with instruments and sensors which started gathering data as soon as the engine was switched on (Dingus, 2006). Data collection system was unobtrusive, and drivers were asked to drive their cars as usual (everyday driving). Sensors were able to collect both data related to vehicle performance and human behaviour, also detecting driver drowsiness, impairments, judgment errors and risk takings. It was also considered an important study because from available data detailed and high-accuracy information on near-crash events were collected. Near-crash situations, indeed, present a couple of benefits with respect to crash events: firstly, they occur more frequently, secondly, they show a successful driver evasive manoeuvre. A major advantage of naturalistic driving study is that video recording allows to view and take into account all of the pre-event and during-event parameters. Another type of studies consists of Field Operational Tests (FOTs): they are testing programmes whose purpose is to get a comprehensive assessment of the efficiency, quality, reliability and acceptance level of Information and Communication Technology (ICT) systems. These, in turn, can be used for smarter, safer, cleaner and more comfortable transport solutions, such as navigation, traffic information and ADAS (FOT-Net, 2010). This includes stand-alone in-car systems as well as cooperative systems. FOTs are a well-known method for manufacturers to look into the way their products are used by the consumer. FOTs are also a step towards the market deployment of mature systems that have proven their functional effectiveness in validation tests with a limited number of test drivers and often on closed test tracks. Over the last decades, a large number of ICT-based transport applications have been successfully developed in research projects throughout Europe. Scenario-based studies have indicated the potential societal benefits of the applications in terms of increased traffic safety, reduced environmental impact and better traffic flow and have discussed the cost-benefit aspects. In general, FOTs can be structured according to the main type of applications tested:

- ADAS – Advanced Driver Assistance Systems (Autonomous Systems)
- Cooperative (Vehicle – Infrastructure) Systems

EuroFOT coordinated a European in-the-field test of driver assistance systems (Kessler et al., 2012). The study focused in particular on eight ADAS that assist the driver in detecting hazards, preventing accidents and making driving more efficient, including:

- Longitudinal control functions (Adaptive Cruise Control, Forward Collision Warning, Speed Regulation System);
- Lateral control functions (Blind Spot Information System, Lane Departure Warning);
- Advanced applications (Curve Speed Warning, Fuel Efficiency Advisor, Safe HMI).

EuroFOT purpose was to quantify the impact of in-vehicle active safety systems on safety, environment, usage and acceptance, and efficiency. Each specific safety system is designed to work in a determined situation, also called use case. Use cases were therefore identified to translate the technical features and specifications of each system into the traffic environment. Participants either owned their test vehicles, leased them during the experiment or took part as professional drivers employed by

freight companies. Data acquisition techniques ranged from questionnaires to continuous recording of vehicle signals, and also, in some cases, additional instrumentation with video and extra sensors. The project started in May 2008 and ended in June 2012. Several hundreds of Terabyte of data have been collected from around 1200 drivers driving for more than 35 million km. The analysis first focused on system performance and user aspects, especially in dangerous situations which could potentially lead to accidents (which have been defined as 'incidents'). This was followed by impact studies on traffic safety, efficiency and environment.

1.4 Driver models

The driver-specific data available from naturalistic driving studies provide a unique perspective from which to test and calibrate driver models. As data storage costs are having a declining trend, collection of data through in-situ vehicles is becoming more and more popular; this leads to a growing need to assess the feasibility of these data for the modelling of driver behaviour. Collected events can be used to calibrate the different developed models, and a comparative analysis to establish which model works best in matching individual drivers and in matching aggregate results can be performed.

Adaptation is one of the most basic survival skills that humans possess that have allowed them to overcome successfully dangerous situations over time (Damasio, 1994). Development of new technologies increases the need of human adaptation constantly: the ability to adapt to such technologies is not trivial as the organism may have limitations regarding the new situation the technology originates. Adaptation and gain compensation by human subjects are related to the complexity of the system to be controlled; the more the complexity, the more the difficulty to control it, the greater the workload and the lower the overall performance. Thus the need of studying how people interact and use the new technology is fundamental for the future success and acceptance of the technology. Cars, in particular, are regarded as one of the biggest mismatches between humans and technology (Vaa, 2001), since they introduced drivers into situations they have never confronted before and that they would have never been exposed without it. Car and driver constitute a complex feedback system. The behaviour of the car results in a certain reaction by the driver. Inversely, the behaviour of the driver affects the behaviour of the car. This "man-machine" system cannot be separated into a purely "mechanical" and a purely "human" component, but must be treated as a whole. When dealing with "human-machine" interfaces, it becomes clear that humans cannot be treated as "linear" elements because they exhibit time delays due to the reaction to stimuli. Other human physical limitations are:

- required processing time for sensed information;
- information transmission time;
- cognitive requirements to anticipate or predict ahead;
- perception of higher derivative information (auditory and haptic information).

The concept of human drivers possessing an "internal model" is linked to the willingness to describe human driver skills in order to estimate the current and future vehicle state, supposing the driver has a basic understanding of the controlled vehicle dynamics.

Understanding the mechanisms and the limitations behind the "human-machine" interface is essential to provide a minimal representation of the human driver. Together with that, an additional set of features may be desirable, even if it is not essential, including:

- neural delays while providing information through sensory channels;
- neuromuscular filtering elements for output channels, such as braking or steering;
- path adjustment strategies to account for driver-related skills in selecting alternative paths;
- adjust speed to facilitate lane keeping along curves, road intersections and driving around obstacles;
- provision of both exceptional and ordinary manoeuvres, in order to discriminate between control responses provided by highly practiced scenarios versus less familiar ones.

1.5 Thesis objectives

Understanding driver's behaviour in intersection is critical for the development of active safety systems for intersections, such as the IDSS. In a project with Volvo Cars, Autoliv and Chalmers, so-called comfort zone boundaries and go/no-go decision timing are to be identified and quantified in order to be used in driver modelling. Some work has been put into identification of such models, but additional efforts are needed. Further identification and implementation of models and evaluation of vehicle parameters to be used in left turn across path driver models are the next steps.
The goal of the thesis is to develop and document an understanding of driver models for left-turn-across path scenarios, including an analysis of human-vehicle interactions. Data recorded during the EuroFOT project were filtered, in order not to include critical manoeuvres for the above stated scenario, and investigated. The work also presumed calibration and tool development for being able to apply and evaluate implemented models on the collected data.
More in detail, two driver models have been examined, with the attempt of finding a link, in one case, between driver behaviour and vehicle dynamics, while in the other one attention has been paid to the relationship between driver behaviour and vehicle speed and acceleration profiles.

2 Literature review

In this chapter, a close look to how researchers investigated the "car-driver" system will be given. A brief introduction about vehicle dynamics and vehicle models will open this chapter, then attention will be paid on two specific driver models: Salvucci and Gray's (Salvucci and Gray, 2004), where driver behaviour is related to the steering wheel angle and the steering wheel angle rate, and Nobukawa's (Nobukawa et al., 2012), which compares speed and acceleration profiles of the vehicle with driver actions/reactions on the gas (or brake) pedal.

2.1 Vehicle dynamics

Vehicle dynamics in its broadest sense encompasses all forms of conveyance, but this report will only refer to road vehicles, paying particular attention to the automobiles. Primary forces by which a high-speed motor vehicle is controlled are developed in four patches where the tyres contact the road. Thus, it becomes important to develop a deep understanding of the behaviour of tyres, characterized by the forces and moments generated over the broad range of conditions over which they operate.
A motor vehicle is made up of many components distributed within its exterior envelope. Anyway, for many elementary analyses, the vehicle can be regarded as one lumped mass concentrated at its centre of gravity (CG) with appropriate mass and inertia properties, as shown in figure 2.1. If the hypothesis of a vehicle as a rigid body can be assumed, the point mass at the CG is dynamically equivalent to the vehicle itself for all motions.

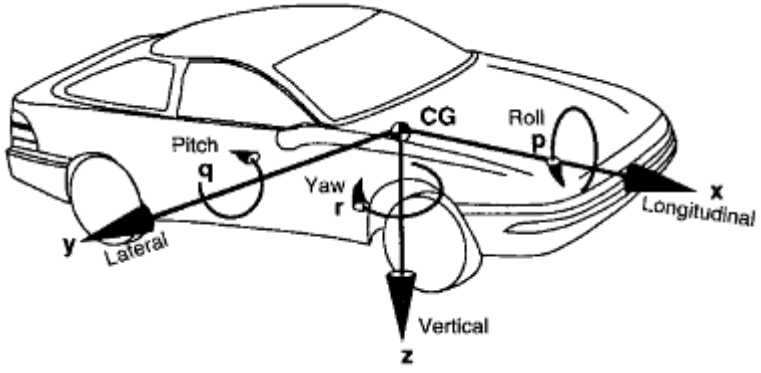

Figure 2.1: SAE Vehicle Axis System

Today, with the computational power available, more complex analyses than the lumped-mass model can be performed: it is possible, indeed, to assemble models for the behaviour of individual components of a vehicle that can be integrated in larger, comprehensive models of the overall vehicle, allowing simulation and evaluation of its behaviour. Such models can provide engineers with a new, powerful tool to test the understanding of a complex system and to solve problems which could not be analysed in the past.

2.1.1 Longitudinal vehicle dynamics

The two major elements of the longitudinal vehicle model are the vehicle dynamics and the powertrain dynamics. The vehicle dynamics is influenced by longitudinal tyre forces, aerodynamic drag forces, rolling resistance forces and gravitational forces (Rajamani, 2005).

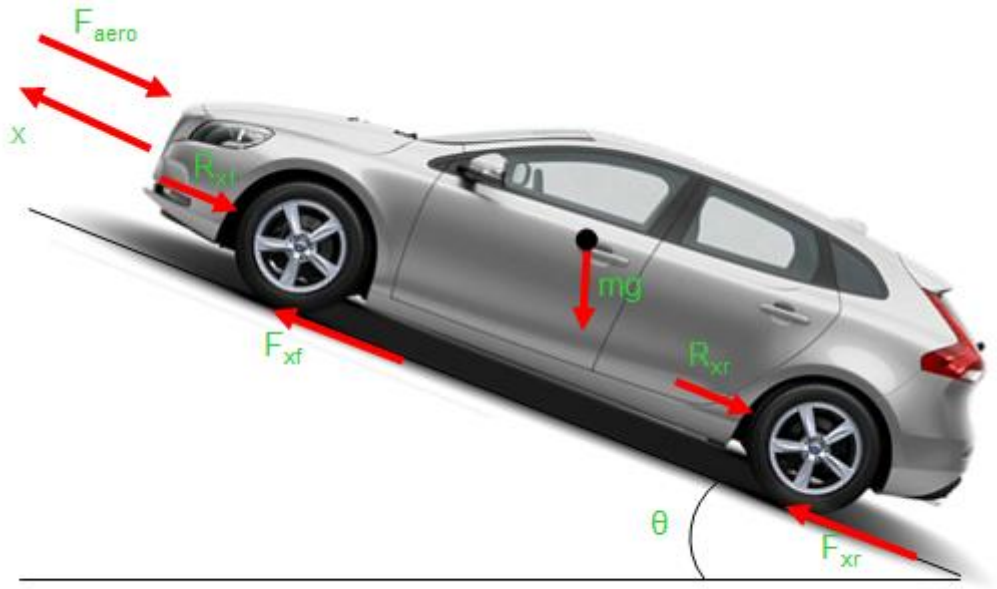

Figure 2.2: Longitudinal forces acting on a vehicle moving on an inclined road

Considering a vehicle moving on an inclined road, as shown in Figure 2.2, a force balance along the vehicle longitudinal axis yields:

$$m \cdot \ddot{x} = F_{xf} + F_{xr} - F_{aero} - R_{xf} - R_{xr} - m \cdot g \cdot \sin(\theta) \qquad (2.1)$$

where F_{xf} is the longitudinal tyre force at front tyres, F_{xr} is the longitudinal tyre force at rear tyres, F_{aero} is the equivalent longitudinal aerodynamic drag force, R_{xf} is the force due to the rolling resistance at front tyres, R_{xr} is the force due to the rolling resistance at the rear tyres, m is the mass of the vehicle, g is the acceleration due to gravity and θ is the angle of inclination of the road on which the vehicle is travelling.
The longitudinal tyre forces F_{xf} and F_{xr} are friction forces from the ground that act on the tyres and they depend on:

- Slip ratio
- Normal load on the tyre
- Friction coefficient of tyre-road interface.

The difference between the actual longitudinal velocity at the axle of the wheel V_x and the equivalent rotational velocity $r_{eff}\,\omega_w$ of the tyre is called longitudinal slip. The equivalent rotational velocity is given by the product between the effective tyre radius (which is different from the nominal one due to tyre deformation in the contact area

with the road) and the wheel angular speed. Longitudinal slip ratio is therefore defined as:

$$\sigma_x = \frac{r_{eff} \cdot \omega_w - V_x}{V_x} \qquad \text{during braking} \qquad (2.2)$$

$$\sigma_x = \frac{r_{eff} \cdot \omega_w - V_x}{r_{eff} \cdot \omega_w} \qquad \text{during acceleration} \qquad (2.3)$$

A rough explanation of why the longitudinal tyre force depends on slip ratio can be seen from Figure 2.3. The upper portion of Figure 2.3 describes the interaction between longitudinal speed and equivalent rotational velocity, while the lower one shows a schematic representation of deformation of the tread elements of the tyre. The tread elements are modelled as a series of independent springs that undergo longitudinal deformation and resist with a constant longitudinal stiffness. Such a model of the tyre is called "brush" model or "elastic foundation" model (Pacejka et al., 1991).

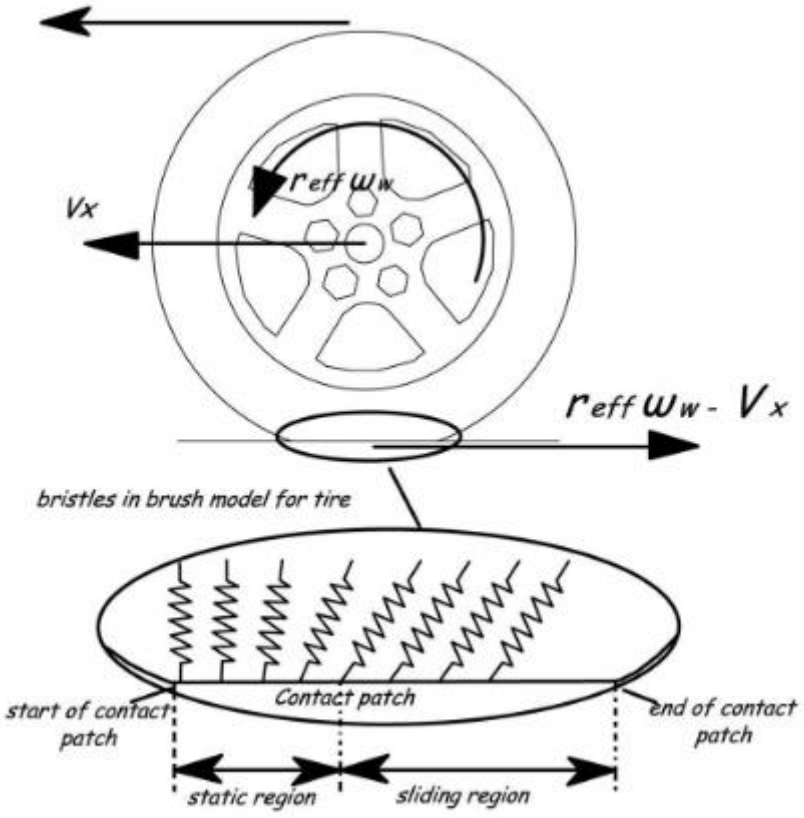

Figure 2.3: Longitudinal force in a driving wheel

As said before, both the tyre and the road are subject to deformation in the contact patch, due to the third law of dynamics (action-reaction principle). While the road deformation can be neglected, the tyre is elastic and so it undergoes deformation. As the tyre rotates, its elastic material is deflected as it goes through the contact patch (compression state) and then springs back to its original shape after it leaves the contact patch itself (extension state). When the tyres are static, then the distribution of

the normal load F, in the contact patch is symmetric with respect to the centre of the contact patch (and of the wheel). However, when the tyres are rotating, the normal load distribution is asymmetric, as shown in Figure 2.4.

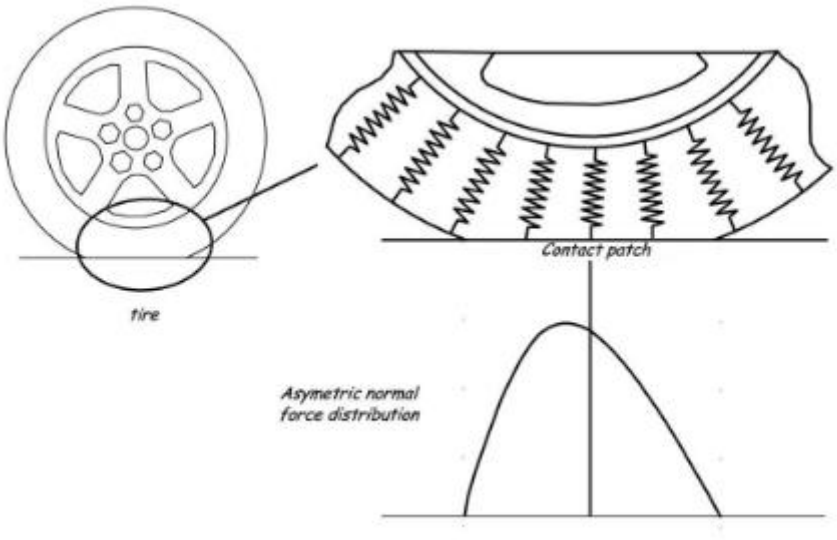

Figure 2.4: Asymmetric normal load distribution on the contact patch

The equivalent aerodynamic drag force on a vehicle can be represented as:

$$F_{aero} = \frac{1}{2} \cdot \rho \cdot C_d \cdot A_f \cdot \left(V_x + V_{wind}\right)^2 \tag{2.4}$$

where ρ is the mass density of air, C_d is the aerodynamic drag coefficient, A_f is the frontal area of the vehicle (projected area of the vehicle in the direction of travel), V_x is the longitudinal vehicle velocity and V_{wind} is the wind velocity (positive for headwind and negative for tailwind).
According to Wang (2004), the frontal area A_f is about 79-84% of the area calculated from the vehicle width and height for passenger cars. As well, the following relationship between vehicle mass m and frontal area A_f can be used for passenger cars with mass in the range 800-2000 kg:

$$A_f = 1.6 + 0.00056 \cdot \left(m - 765\right) \tag{2.5}$$

Finally, the aerodynamic drag coefficient C_d can be roughly determined from a coast-down test (White et al., 1972). In a coast-down test, the vehicle is launched at an initial speed, the throttle angle is kept at zero and the vehicle is allowed to slow under the effects of aerodynamic drag and rolling resistance.
Due to the internal damping of the tyre material, after the tyre section, which has undergone the contact patch forces, has left the contact area, rubber material is not able to completely recover to its original state and shape. This loss of energy can be represented by a force on the tyres called the rolling resistance that acts to oppose the motion of the vehicle. The loss of energy in tyre deformation also results in a non-symmetric distribution of the normal tyre load over the contact patch (which explains the asymmetric load distribution in Figure 2.4).

The rolling resistances R_{xf} and R_{xr} are typically modelled as being roughly proportional to the normal force on each set of tyres i.e.:

$$R_{xf} + R_{xr} = f \cdot \left(F_{zf} + F_{zr}\right) \tag{2.6}$$

where f is the rolling resistance coefficient. To see why this approximation is made for the rolling resistance force, the action of the normal load and rolling resistance force shown in Figure 2.5 has to be considered. The value of the rolling resistance coefficient f varies in the range 0.01 to 0.04. A value of 0.015 is typical for passenger cars with radial tyres (Wang, 2004).

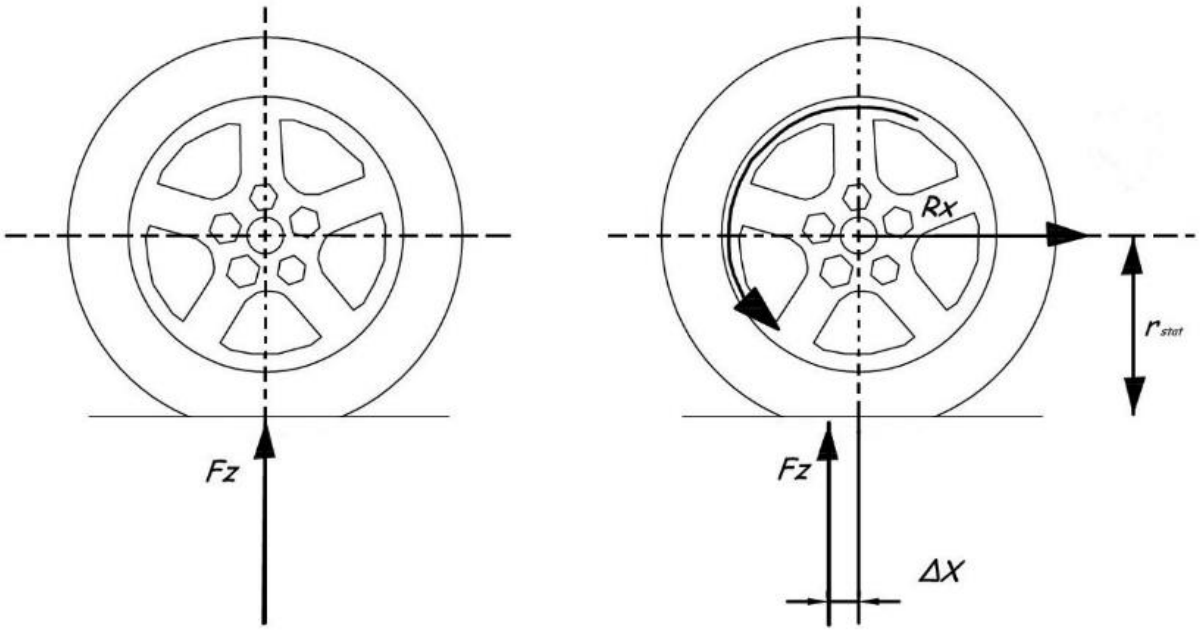

Figure 2.5: Description of rolling resistance for not rotating (left) and rotating (right) wheel

2.1.2 Lateral vehicle dynamics and bicycle model

When a vehicle drives through a curve, lateral forces are needed for course holding and lateral slips occur at the wheels. When dealing with slowly-moving vehicles, such lateral forces can be neglected as their value is very low and, in that case, the most appropriate and simple model to use is the one-Degree-Of-Freedom (one-DOF) bicycle model: the front and rear wheels are represented, respectively, by one central front and rear wheel and the vehicle is assumed to have planar motion with only vehicle kinematics involved. The necessary steering angle of the front wheels can be constructed via given momentary turning centre through the Ackermann geometry (Rill, 2003). The major assumption used in the development of such kinematic model is that the slip angles at both wheels must be equal to 0 that is a reasonable assumption only for low-speed motion of the vehicle (less than 5 m/s).
Since the entire report is dealing with urban speeds (therefore, higher speeds than 5 m/s), such model can't be representative for the conducted analysis (Rajamani, 2005). Instead, a more complex "bicycle" model of the vehicle with two DOF can be considered, as shown in Figure 2.6. The two degrees of freedom are represented by the vehicle lateral position y and the vehicle yaw angle ψ. The vehicle lateral position

is measured along the lateral axis of the vehicle to the point O which is the centre of rotation of the vehicle. The vehicle yaw angle ψ is measured with respect to the global axis X. The longitudinal velocity of the vehicle at the CG is denoted by V_x.

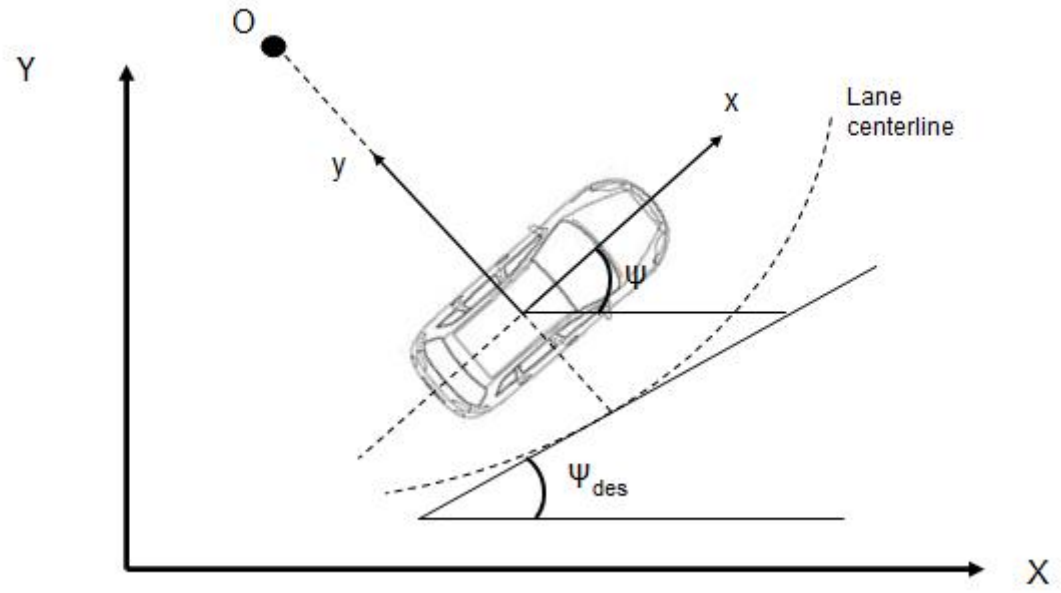

Figure 2.6: Lateral vehicle dynamics

Ignoring road bank angle that is not the primary aim of this study, by applying Newton's second law for motion along the y-axis:

$$m \cdot a_y = F_{yf} + F_{yr} \tag{2.7}$$

where a_y is the inertial acceleration of the vehicle at the CG in the y-direction and F_{yf} and F_{yr} are the lateral tyre forces of the front and rear wheels respectively. Two terms contribute to a_y value: the acceleration $\ddot{y}$ which is due to motion along y-axis and the centripetal acceleration $V_x\dot{\psi}$. Hence

$$a_y = \ddot{y} + V_x \cdot \dot{\psi} \tag{2.8}$$

Substituting from equation (2.8) into equation (2.7), the equation for the lateral translational motion is obtained as

$$m \cdot \left(\ddot{y} + V_x \cdot \dot{\psi}\right) = F_{yf} + F_{yr} \tag{2.9}$$

Moment balance about the z-axis yields the equation for the yaw dynamics as

$$I_z \cdot \ddot{\psi} = l_f \cdot F_{yf} - l_r \cdot F_{yr} \tag{2.10}$$

where l_f and l_r are the distances of the front tyre and the rear tyre respectively from the CG of the vehicle. The next step is to model lateral tyre forces F_{yf} and F_{yr} that act on the vehicle. From experimental results (Rajamani, 2005), which show that there is a direct proportionality between the lateral tyre force and the slip angle for small slip angles, it has been possible to establish the parameters which affect such values:

$$F_{yf} = 2 \cdot C_{\alpha f} \cdot \alpha_f = 2 \cdot C_{\alpha f} \cdot \left(\delta - \theta_{Vf}\right) \quad (2.11)$$

$$F_{yr} = 2 \cdot C_{\alpha r} \cdot \alpha_r = 2 \cdot C_{\alpha r} \cdot \left(-\theta_{Vr}\right) \quad (2.12)$$

where $C_{\alpha f}$ and $C_{\alpha r}$ are, respectively, the cornering stiffness of each front and rear tyre, α_f and α_r are the slip angles for the front and rear wheels, δ is the front wheel steering angle and θ_{Vf} and θ_{Vr} the front and rear tyre velocity angle. The factor 2 accounts for the fact that this model takes into account two front and rear wheels. With respect to the slip angle, it is defined as the angle between the orientation of the tyre and the orientation of the velocity vector of the wheel, as depicted in Figure 2.7.

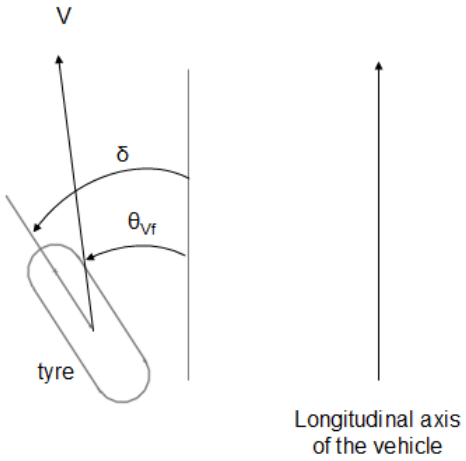

Figure 2.7: Front tyre slip angle

Using small angle approximations, it is possible to define θ_{Vf} and θ_{Vr} through the following equations:

$$\theta_{Vf} = \frac{\dot{y} + l_f \cdot \dot{\psi}}{V_x} \quad (2.13)$$

$$\theta_{Vr} = \frac{\dot{y} - l_r \cdot \dot{\psi}}{V_x} \quad (2.14)$$

2.1.3 Other vehicle dynamics models

Most of reference models for chassis controls usually have low level DOF like the bicycle model and, in some cases, these models can be not accurate enough. Then, models with higher level DOF (like multi-body dynamic models) were created but they present long solving times and, therefore, are not appropriate for real time analysis to use (Lee et al., 2008). However, as a reference, those complex models will be introduced in the next sections.

2.1.3.1 Horizontal vehicle model

The horizontal vehicle model considers 3 DOF and it consists of longitudinal, lateral translation, and rotation of vehicle mass centre, as shown in figure 2.8.

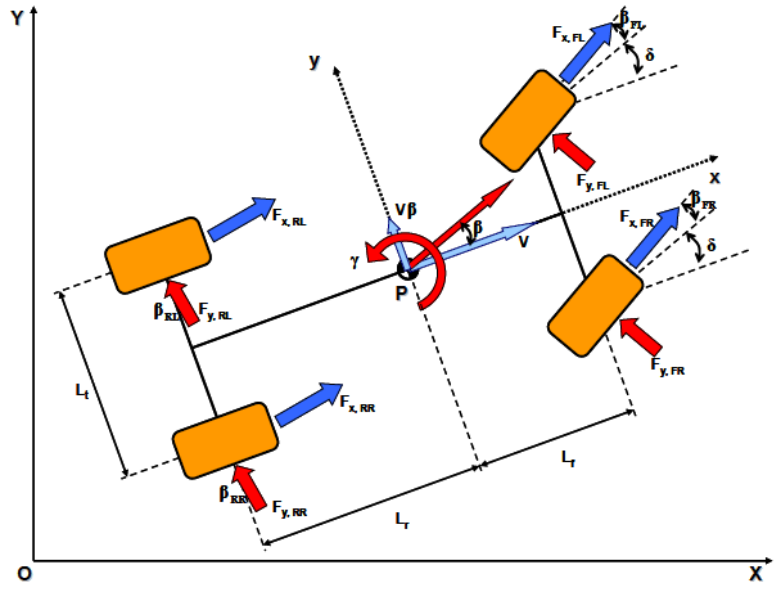

Figure 2.8: 3 DOF horizontal vehicle model

The equations which perfectly describe the system are the following ones:

$$m \cdot \ddot{x} = F_{x,FL} + F_{x,FR} + F_{x,RL} + F_{x,RR} \tag{2.15}$$

$$m \cdot \ddot{y} = F_{y,FL} + F_{y,FR} + F_{y,RL} + F_{y,RR} \tag{2.16}$$

$$I_{ZZ} \cdot \dot{\gamma} = L_F \cdot \left(F_{y,FL} + F_{y,FR}\right) - L_R \cdot \left(F_{y,RL} + F_{y,RR}\right) \tag{2.17}$$

The meaning of each symbol of the formulas is described in table 2.1. The subscripts FL, FR, RL and RR indicate respectively front-left, front-right, rear-left and rear-right.

Table 2.1: Horizontal vehicle model symbols

Symbol	Parameter
M	Vehicle total mass
$\ddot{x}$, $\ddot{y}$	Longitudinal axis acceleration, Lateral axis acceleration
F_x, F_y	Longitudinal and Lateral force at each tyre
L_F, L_R	Front and Rear wheel base
I_{ZZ}	Vertical axis moment of inertia
$\dot{\gamma}$	Yaw angular acceleration

2.1.3.2 Vertical vehicle model

The vertical vehicle model is made of 7 DOF, as represented in Figure 2.9. This model takes into account two dimensions for vertical dynamics, one track half car model for pitch dynamic and two track half car models for roll dynamic. Overall, the model has 3 DOF at mass centre (vertical, roll, pitch dynamics) and 1 vertical DOF at each wheel.

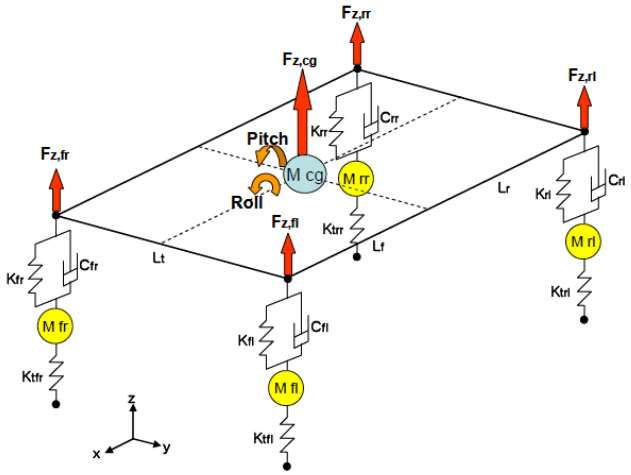

Figure 2.9: 7 DOF vertical vehicle model

The vertical dynamic equations which represent the system are:

$$m_S \cdot \ddot{z} = F_{Z,FL} + F_{Z,FR} + F_{Z,RL} + F_{Z,RR} + \frac{M_{\theta,F}}{L_F} - \frac{M_{\theta,R}}{L_R} \tag{2.18}$$

$$I_{yy} \cdot \ddot{\theta} = -L_F \cdot F_{Z,FL} - L_F \cdot F_{Z,FR} + L_R \cdot F_{Z,RL} + L_R \cdot F_{Z,RR} + M_{\theta,F} + M_{\theta,R} \tag{2.19}$$

$$I_{xx} \cdot \ddot{\phi} = 0.5 \cdot L_T \cdot F_{Z,FL} - 0.5 \cdot L_T \cdot F_{Z,FR} + 0.5 \cdot L_T \cdot F_{Z,RL} - 0.5 \cdot L_T \cdot F_{Z,RR} + M_{\phi,L} + M_{\phi,R} \tag{2.20}$$

$$m_U \cdot \ddot{z}_{U,FL} = F_{Z,FL} - 0.5 \cdot \frac{M_{\theta,R}}{(L_F + L_R)} + 0.5 \cdot \frac{M_{\phi,R}}{L_T} + F_{T,FL} \tag{2.21}$$

$$m_U \cdot \ddot{z}_{U,FR} = F_{Z,FR} - 0.5 \cdot \frac{M_{\theta,R}}{(L_F + L_R)} - 0.5 \cdot \frac{M_{\phi,L}}{L_T} + F_{T,FR} \tag{2.22}$$

$$m_U \cdot \ddot{z}_{U,RL} = F_{Z,RL} + 0.5 \cdot \frac{M_{\theta,F}}{(L_F + L_R)} + 0.5 \cdot \frac{M_{\phi,R}}{L_T} + F_{T,RL} \tag{2.23}$$

$$m_U \cdot \ddot{z}_{U,FL} = F_{Z,RR} + 0.5 \cdot \frac{M_{\theta,F}}{(L_F + L_R)} - 0.5 \cdot \frac{M_{\phi,L}}{L_T} + F_{T,RR} \tag{2.24}$$

Table 2.2 collects all the symbols used in the previous equations.

Table 2.2: Vertical vehicle model symbols

Symbol	Parameter
m_S, m_U	Sprung and Unsprung mass
$\ddot{z}$, $\ddot{z}_U$	Vertical acceleration at sprung mass and unsprung mass
I_{xx}, I_{yy}	Longitudinal and Lateral axis moment of inertia
$\ddot{\theta}$, $\ddot{\phi}$	Pitch and Roll axis angular acceleration
$F_{Z,FL}$, $F_{Z,FR}$,$F_{Z,RL}$, $F_{Z,RR}$	Vertical force at each suspension
$F_{T,FL}$, $F_{T,FR}$, $F_{T,RL}$, $F_{T,RR}$	Vertical force at each tyre

2.2 Driver models

During the driving task, vehicle dynamics and road environment are relevant aspects, but also the drivers' emotional and motivational factors play an important role. Then, in order to model driver's manoeuvres, it is important to have reliable drivers' models that can take into account human behaviour during the driving task, although this is not simple. A lot of research has been conducted during the last decades on driver models, but most existing models just work in very particular scenarios and with specific limitations. Most driver models also only include a subset of all possible variables that can influence drivers' behaviour, in a majority excluding explicit motivational and driver internal state factors, while representing the effect of such factors through data driven models (Cacciabue , 2007).

When dealing with drivers' modelling, it is important to consider that driving is a self-paced task in which drivers' actions are influenced by different human characteristics such as emotions, feelings, concentration and experience (Naatanen and Summala, 1974). Hence, driver's behaviour should be included in manoeuvres modelling in order to make them and the overall driving task more accurate and realistic. An essential property of drivers' models is its easiness to use and the possibility of its further implementation and integration within ADAS or part of evaluation of other parts of system designs.

Over the years, different theories on human behaviour led to different drivers' models. Some researchers argued that drivers seek some specific target feelings during the driving task and, in order to reach them, they adapt their way of driving. A link between driving and tension or anxiety has been found by Taylor who related the galvanic skin response (GSR) measured on 20 drivers to the level of tension or anxiety that the driver was willing to accept (Taylor, 1964). Several researchers developed theories to describe the factors that affect humans' choice to drive in a specific way. For example, Wilde's "Risk homeostasis" theory (RTH) states that the driver seeks a certain constant level of risk while driving and that this level of risk should be perceived as a number (Wilde, 1982), as shown in the block diagram of Figure 2.10.

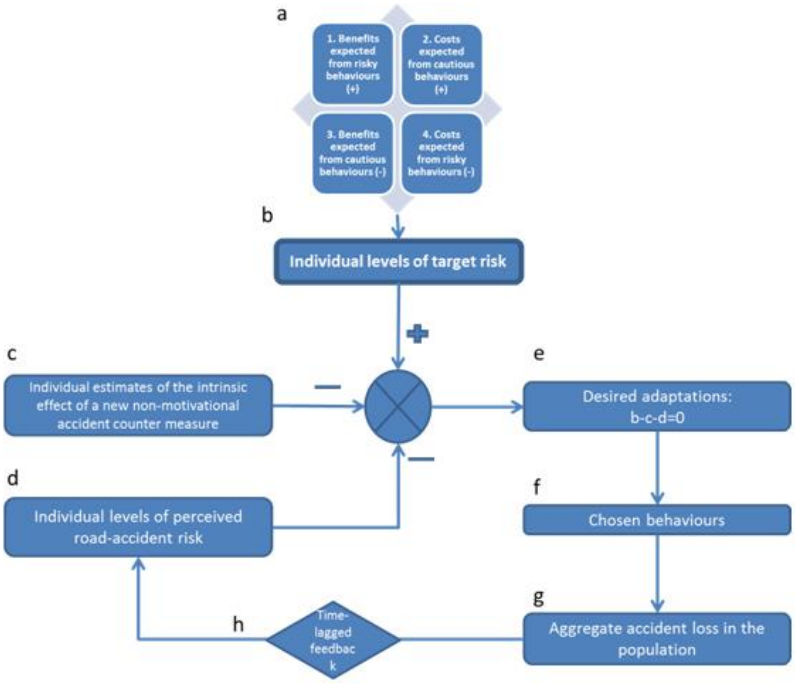

Figure 2.10: Wilde's model of risk homeostasis

Wilde introduced a comparator where the targeted level of risk, *b*, is compared with the individual estimate of the intrinsic effect of a new non-motivational road safety measure, *c*, and the individual level of perceived road accident risk, *d*. The output of the comparator, *e*, corresponds to the desired adaptation that satisfies the formula of the RHT and its value is assumed to be equal to 0 (Wilde, 1982):

$$b - c - d = 0 \qquad (2.25)$$

It has been criticized those parameters don't exist in reality, as there is no evidence or study supporting this theory; moreover, even though they existed, drivers would calculate them unconsciously and there would be no possibility to test the hypotheses related to the model (Cacciabue, 2007).
On the other hand, the 'zero risk model', proposed by Naatanen and Summala (1974), posits that the driver acts in order to reach a zero risk level.
Safety margins are also mentioned to be vital in driver's task control and decision making and they can be seen, whether the car is in motion or not, as comfort zone, with no threat, risk, or discomfort felt by the driver (Naatanen &Summala, 1974; Summala 1988).
An alternative (or complementary) approach exists based on Damasio's somatic marker hypothesis which focuses more on physiological and neurological aspects (Damasio, 1994). In his "Monitor Model", Damasio sees drivers as persons whose most basic instinct is survival and acting according to that instinct. The monitor model he proposes contemplates the body as the monitor and states that its main objective is to survive using specialized skills that he masters for that purpose. In this case the main objective of the monitor (body) is to achieve a target feeling while driving. Driver emotions and feelings are in this model separated and trigger monitor actions in order to achieve a target feeling desired by the driver. Emotions are unconscious responses activated by external factors and feelings can be described as the conscious perception of body states, also activated by external stimuli.

The models described up to now give a general overview on drivers' motivations and feelings but do not describe in detail drivers' behaviour with respect to manoeuvring (e.g., steering, turning). Other models have been developed for this scope during last decades. Regarding steering behaviour, it is acknowledged that the drivers require visual inputs from the environment or the road in front of the vehicle's present heading, at some "preview" distance (Salvucci & Gray, 2004).

Donges introduced a two-level model of steering in which he contemplates two complementary loops, an "anticipatory closed-loop control" mechanism combined with a "compensatory closed-loop control" sub-model (Donges, 1978). The first level anticipates the desired path curvature with the information provided by visual information obtained from the road and the second one reacts to the different error outputs and compensates the trajectory. The final output of the model is the resulting steering wheel angle of the car.

A further study (Land & Lee, 1994) showed clearly that drivers mainly looked at the tangent point inside of each bend (being the tangent point the visual point on the inside lane edge or road shoulder where the apparent orientation of the curve is reversed), during normal driving in winding roads (Land & Lee, 1994). Later, an experiment was conducted (Land & Horwood, 1995) to illustrate that drivers do not use as input only one visual region of the road but, instead, different parts of the road. In their driving simulator based research, Land and Horwood showed to the drivers only some small slices of the road, from far and near regions in front of the car. As a result, they found that the driver steering accuracy was higher when both segments from the near and far point were visible at the same time and, in this situation, the best steering performance was achieved (Land & Horwood, 1995).

Human estimations accuracy and capabilities also was a researched topic. Fildes and Triggs conducted an experiment in order to study the effects of independent curve variables, such as curve radius, curve angle and so on, on subjects' magnitude predictions of road curvature using perspective computer generated line drawings (Fildes & Triggs, 1995). Subjects were found to underestimate road curvature and predictions made where found to be estimated using the curve deflection angle which is not a good estimator for road curvatures, as for the same deflection angle we can obtain different road curvatures depending on the radius.

Driver models for intersection traversing have different approaches; some are based on modelling the speed as the model from Liebner et al. (2013) that focuses on the velocity profile of the vehicle approaching an intersection. Also, the Nobukawa et al. approach proposes an anticipatory speed control model (Nobukawa et al., 2012) that does not only includes the approach stage but also the turning stage and targets both the vehicle speed and the lateral and longitudinal accelerations. However, in this model, the main objective is to obtain the moment in which the driver decides to turn by calculating the desired accelerations the driver seeks. Another model is the one proposed by Asano et al. (2010) in which they model the vehicle trajectory during the left turn considering the geometry of the intersection. On the other side, models regarding drivers' behaviour during the turn are few and don't include the full turn or just emphasises on the approach stage or the actions undertaken by the driver when facing the manoeuvre. Akamatsu et al. (2003) studied the driver behaviour when approaching the intersection applying the Bayesian network, which consists of a probabilistic graphical model, to the variables of the behavioural event. Furthermore, Aoude et al. (2011) research on driver behaviour classification by developing algorithms estimating driver behaviour at road intersections based on two models: support vector machines and hidden Markov models. As its possible to notice more

research is needed in that field and for our thesis purpose the intention of implementing both driver behaviour and vehicle dynamics models would be addressed during the left turn stage.

2.2.1 Salvucci and Gray: a two-point visual control model for steering

In their steering control model study, Salvucci and Gray remarked that previous presented models had some limitations (Salvucci and Gray, 2004). For example, they found incoherence between the work of Land and Lee (1994) and the work of Fildes and Triggs (1995). In the former, it was stated that the driver estimates the road curvature using the tangent point whereas, in the latter, the authors point out that this humans-made estimation is inaccurate.
As a result, Salvucci and Grey presented a straightforward computational two-level (two points) model that was validated using the data acquired by Land and Horwood (1995). Those data were acquired in a simulator study where drivers were performing a normal driving task in a single lane road with no other vehicles and, thus, the model was only evaluated for this case scenario. Further, the model was tested with only 3 different drivers been driver differences and characteristics not taken in account when evaluating the results. As a model including driver behaviour their characteristics should be included in it somehow. For that matter, as explained in the next section, the model implemented by Salvucci and Gray considers different parameters describing the drivers' characteristics.

2.2.1.1 Near and far points

The principal novelty of the model developed by Salvucci and Grey is that it explicitly includes two particular points, named "near point" and "far point" that are stated to be used by the driver during steering (Salvucci & Gray, 2004). The "near point" is a fixed point in front of the heading of the vehicle at a distance "near enough to monitor lateral position and far enough that the driver can comfortably see the region through the windshield". In turn, the "far point" is represented by "some salient distant point with which the model can monitor lateral stability and given the distance maintain a predictive steering angle that compensates for the upcoming road profile". From the definition, the near point and the far point play different roles when steering: the near point is used by the driver to monitor lateral position while the far point monitors lateral stability. The different near and far regions where the points are located complement each other and their combination allows the driver to perform a good steering while driving (Land & Horwood, 1995). It is relevant to highlight that the near point remains at a fixed distance while the far point can vary depending on the situation, road characteristics and surroundings (a distant point in the horizon, a tangent point in a curve or a leading car are some common options to represent the far point), as it can be seen in Figure 2.11.

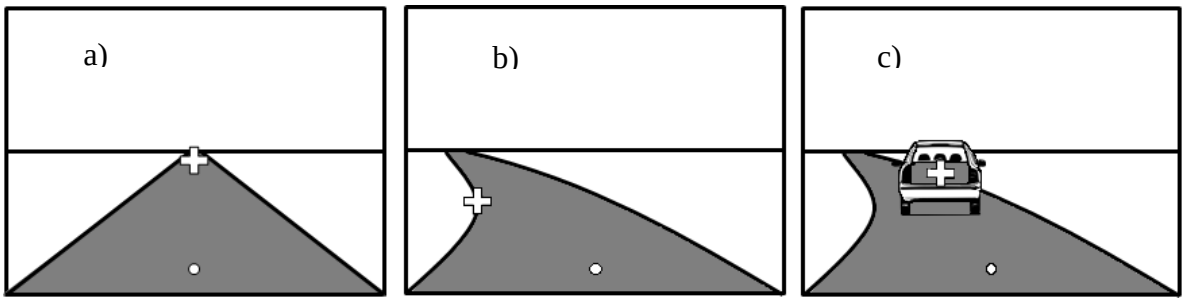

Figure 2.11: Near and far points for three scenarios (a) straight roadway with vanishing point, (b) curved roadway with tangent point, (c) presence of lead car

2.2.1.2 Model equations and definition of parameters

Starting from a standard proportional integral controller, Salvucci and Gray (2004) proposed a steering control law based on the existence of the near and far points:

$$\varphi = k_p \cdot \theta + k_I \cdot \int \theta dt \tag{2.26}$$

In the above equation (2.26), φ represents the steering wheel angle of the vehicle which is the parameter desired to be calculated. θ is the angle between drivers heading direction and the direction of the desired target point which in our case will represent the error that the driver constantly tries to minimize. The coefficients k_p and k_I correspond to the constants that scale the proportional and integral terms respectively. The derivative form, which is easier to use, is given by:

$$\dot{\varphi} = k_p \cdot \dot{\theta} + k_I \cdot \theta \tag{2.27}$$

The equation is then reformulated including the near and far visual points represented in the equation (2.28) by θ_n and θ_f, the visual direction to the near and far points correspondingly. The following equation calculates the steering wheel angle rate at each time interval:

$$\dot{\varphi} = k_f \cdot \dot{\theta}_f + k_n \cdot \dot{\theta}_n + k_I \cdot \theta_n \tag{2.28}$$

In this case, the proportional variation of θ is divided in two terms. In the new terms, $\dot{\theta}_n$ and $\dot{\theta}_f$ represent the variation in, respectively, the near and far points visual directions, in which they are regulated by the coefficients k_n and k_f. Also the second term in equation (2.27), corresponding to the integral term of the visual direction of the desired target, is modified to represent only the visual direction of the near point as it reflects better the current lateral position error of the vehicle. The model then tries to constantly adjust the stability of the near and far point $\dot{\theta}_n$ and $\dot{\theta}_f$, the near point to maintain the car in the middle of the lane and the far point to ensure a good predictive steering angle, as shown in Figure 2.12.

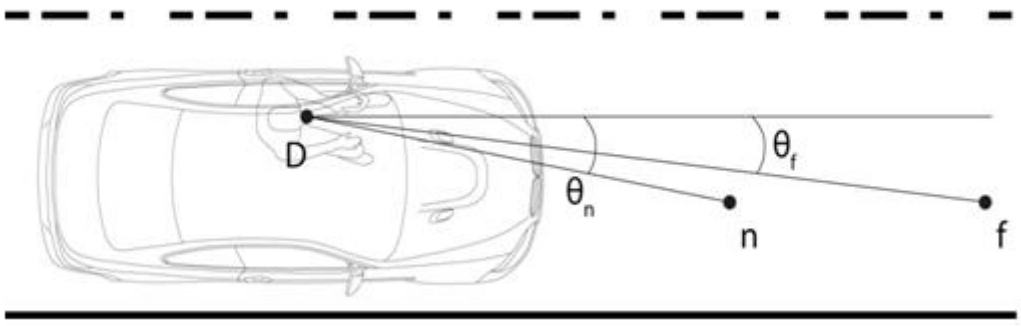

Figure 2.12: D, n and f represent respectively the driver and the near and far points located in the front of the car. θ_n and θ_f represents the angle between drivers heading direction and the direction of the desired target point respectively

The three coefficients (k_n, k_f, k_I) will vary depending on the driver and the situation. If the driver has a more or less aggressive style, his/her behaviour will be reflected in those parameters. The model was then tested to check if it steered as expected and it was compared to empirical data. In particular, three different steering validation studies were conducted: "curve negotiation", "corrective steering" and "lane-changing", in which the model obtained major drivers behaviours pretty accurately as a result.

Following up Salvucci and Gray work, Benderius (2013) adapted the steering model to a new scenario. This new situation differed from the one proposed by Salvucci and Gray in one main feature: the driver was not involved in a normal driving situation but instead the manoeuvre consisted of a corrective steering action in a critical situation. The car initial position was located outside the desired lane path (some deviation existed initially on the y axis) with the heading of the car not aligned with the road direction and, therefore, the heading angle (angle between the heading of the vehicle and the road direction) differed from zero (Figure 2.13). The driver faced a critical situation and was required to steer drastically to get back to the normal, expected position, which belongs to the desired comfort zone he is seeking.

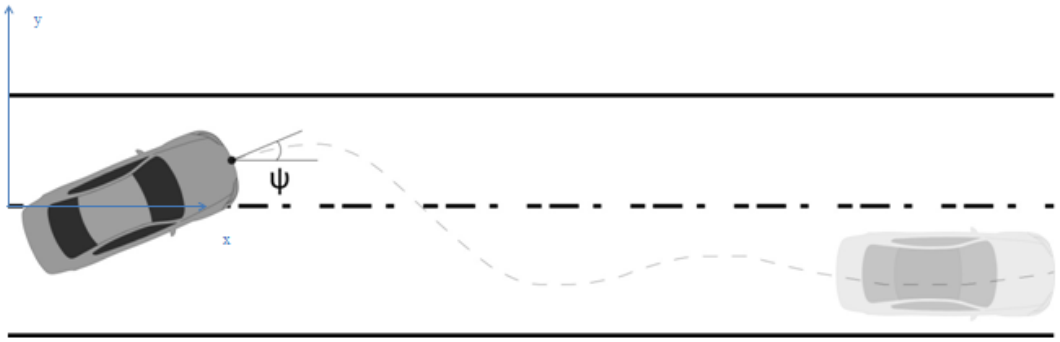

Figure 2.13: The car starts on the opposite lane at a positive value y with a specific heading angle Ψ and then steers back until the desired normal lane position, trajectory represented by the dotted line

The model implemented by Benderius (2013) demonstrated to have a relatively high correlation with the empirical data and, therefore, it seemed to perform quite well in this scenario.

In this thesis work, starting from the Salvucci and Gray approach and the further work performed by Benderius, a model will be implemented for a particular scenario, which

already has been described in the "Introduction": the left turn across path/opposite direction (LTAP/OD).

2.2.2 Nobukawa's model

Driver's perception of vehicle acceleration is a primary factor which directly influences vehicle speed control. With respect to that, in an ordinary manoeuvre like turning left, the driver can choose between two possible outcomes: braking to stop before passing the intersection if there is no sufficient gap (due to an oncoming vehicle) or reducing the speed to ensure a comfortable left turn. Many researchers consider drivers to have mental model of the driving situation, which is continuously updated based on current vehicle speed and distance from the intersection, that are created inside driver's mind as part of the driving task and decision making process (Nobukawa et al., 2012). Nobukawa bases his longitudinal control model on this assumption, but what distinguishes his work from his is that he also included additional consideration due to lateral control. In this way, the driver has to simultaneously address multiple potential outcomes, once a set of stimuli through the five senses has been perceived.
The overall left turn manoeuvre can be divided into three stages: an approach stage, where speed is reduced and lateral acceleration is small, a turning stage, where lateral acceleration is dominant respect to the longitudinal one, and an exit stage, which corresponds to the vehicle accelerating again and leaving the intersection.
In a left turn intersection, the dominant factor during the straight-line approach is supposed to be the mental anticipation of the accelerations required to either make the turn or stop before making the turn itself. According to Nobukawa's approach, the longitudinal control of the vehicle, during the left turn, can be modelled through the human-vehicle model represented in the block diagram of Figure 2.14. The vehicle is represented by two boxes, where longitudinal vehicle dynamics is able to provide the real longitudinal acceleration a_x and the speed U, while the lateral dynamics, together with a speed control model, provides the desired longitudinal acceleration a_x^{des} as output. The difference in value between the desired acceleration a_x^{des} and the real longitudinal acceleration a_x is perceived (with a time delay τ) by the driver, who acts on the gas or brake pedal (u_x) in order to, respectively, increase or decrease the longitudinal acceleration, getting its value closer to the desired one.

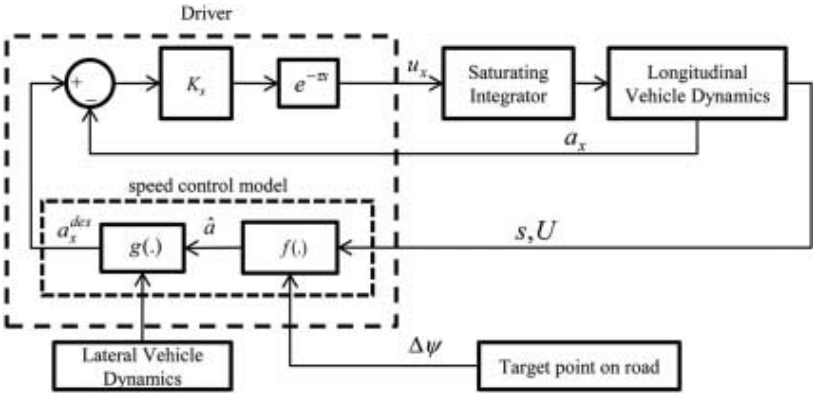

Figure 2.14: Nobukawa's driver-vehicle model

The most relevant aspect of Nobukawa's model is that the driver's control of speed during a left turn is based on the anticipation of the longitudinal and lateral

accelerations. Those longitudinal and lateral anticipated acceleration references (AAR), respectively named $\hat{a}_x$ and $\hat{a}_y$, play an important role to evaluate the desired longitudinal acceleration a_x^{des}. The expression used to calculate $\hat{a}_x$ and $\hat{a}_y$ includes s to represent the longitudinal position of the vehicle on its path. The severity of the turn is represented by the change in heading angle, $\Delta\psi$, approximately 90° for left turns, as it is given from the difference between the current value ψ and a future value ψ_Q, where Q is the target point chosen by the driver (located at the end of the turning stage), also called gaze point (Figure 2.15).

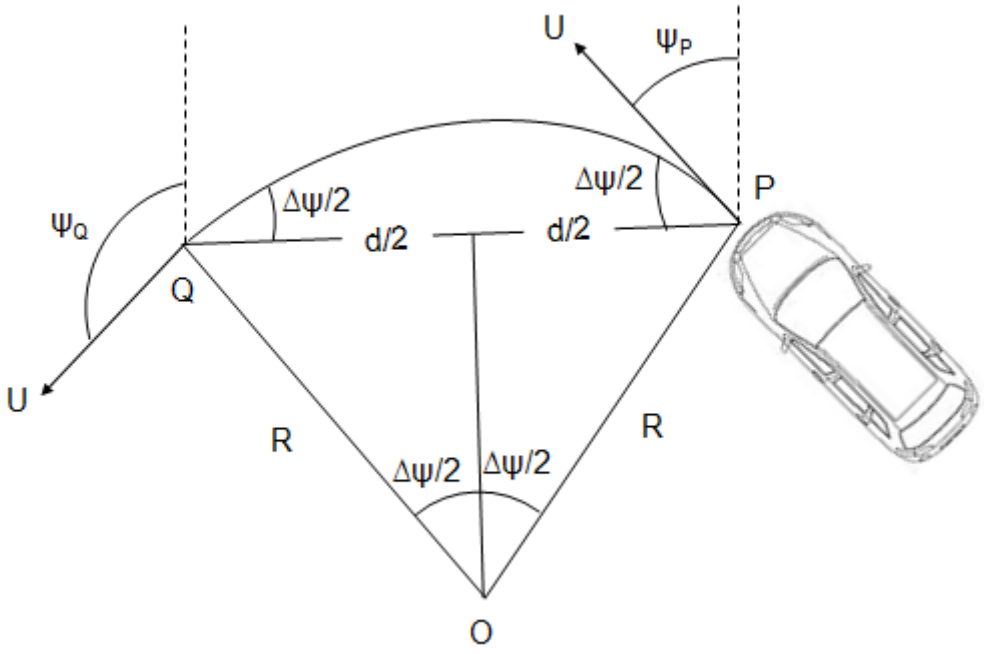

Figure 2.15: Geometry for the calculation of â based on circular path and constant speed

Based on an assumed constant rate of turn, it is possible to obtain the reference anticipated lateral acceleration with on the following equation:

$$\hat{a}_y = \frac{U^2}{R} = \frac{2 \cdot U^2 \cdot \sin\left(\frac{|\Delta\psi|}{2}\right)}{d} \tag{2.29}$$

where d is the distance between the actual vehicle position and the target point and R is the curvature radius. Even if d (and R as a consequence) can change over time, it can be assumed for simplicity that the selection of point Q is done so that a constant radius path is feasible. Nobukawa hypothesises that there is no expectation the driver computes this formula in his mind, but instead that, based on his/her experience, the driver will build a corresponding associative map between the visual stimulus derived from U, $\Delta\psi$, d and the response $\hat{a}_y$.

Regarding the longitudinal acceleration, Levison presented a stopping distance model where the driver is assumed to predict the constant acceleration required to brake to rest (Levison et al., 1998). As such, the longitudinal acceleration computed by Levison can be considered as the anticipated longitudinal acceleration and calculated by using the following equation:

$$\hat{a}_x = \frac{U^2}{2 \cdot d} \tag{2.30}$$

Comparing equations (2.29) and (2.30), the two anticipated accelerations become equal for a particular change in heading angle:

$$\frac{2 \cdot U^2 \cdot \sin\left(\frac{|\Delta\psi|}{2}\right)}{d} = \frac{U^2}{2 \cdot d} \qquad \text{which, simplifying, leads to} \quad |\Delta\psi| \approx 29° \tag{2.31}$$

The point where, during the intersection approach stage, $\hat{a}_x = \hat{a}_y$, is called crossover point. Before such point the driver has not decided yet if to stop before the intersection or to pass through it and therefore he/she controls the longitudinal acceleration ($\hat{a}_x$ dominant over $\hat{a}_y$). After such point the decision has been taken and, assuming that the driver has decided to turn (no obstacles at the intersection), $\hat{a}_y$ provides the unique reference for the speed control ($\hat{a}_y$ dominant over $\hat{a}_x$).
The value of the desired longitudinal acceleration a_x^{des} is computed through the control function g(.), as shown in Figure 2.14. During the approach and turn stage, g(.) becomes a piecewise-linear control function that describes a_x^{des} as a function of the anticipated accelerations (Figure 2.16). At the beginning of the approach stage, it is assumed the driver is not pushing on the gas pedal, generating a gentle coast-down deceleration a_0. Coast-down deceleration is obtained from the following equation:

$$a_0(U) = c_1 + c_2 \cdot U + c_3 \cdot U^2 \tag{2.32}$$

When a certain $\hat{a}$ threshold, called lb_1 in Figure 2.16, is reached, the driver presses on the brake pedal and a deeper deceleration is applied. Therefore, in the approach stage, the a_x^{des} is a function of the longitudinal anticipated acceleration, whereas during the turning stage the a_x^{des} is a function of the lateral acceleration (anticipated $\hat{a}_y$ or actual $|\hat{a}_y|$). Finally, during the exit stage, the a_x^{des} is considered equal to a constant a_3.
In order to calculate the desired longitudinal acceleration of the vehicle in the different stages (approach, turn and exit), the Nobukawa's approach requires to estimate the four parameters which describe a_x^{des} in the three different stages (a_0 and a_1 for the approach stage, a_2 for the turn stage and a_3 for the exit stage), together with the lower and upper boundaries (lb_1 and ub_1 for the approach stage and lb_2 and ub_2 for the turn stage). The procedure used to obtain the parameters for the turning stage will be outlined later in chapter 3.

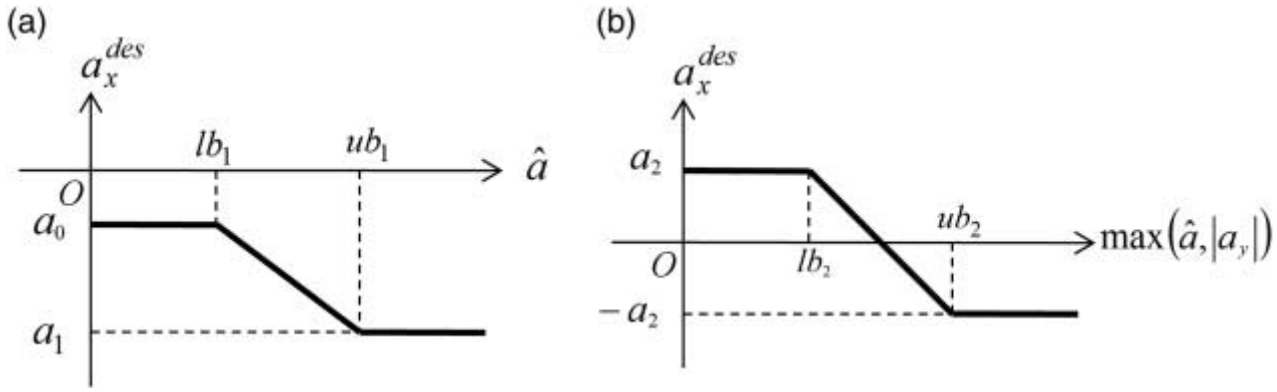

Figure 2.16: Nonlinear control function g(.) for (a) approach stage (b) turn stage

Comparison between measurements and fitted model must be performed, and the root mean square error for both speed and longitudinal acceleration is calculated. As indicated by Nobukawa et al. (2012), the RMSE should rarely exceed the value of 1 m/s and 1 m/s^2, respectively for speed RMSE and longitudinal RMSE. RMSE values higher than 1 indicate, indeed, that the left turn manoeuvre has not been performed in an ordinary way: extraneous factors, like visual distractions or driver impediments have affected the overall event.

3 Method

In this section it is explained what kind of parameters were extracted from Naturalistic Driving Studies in order to perform the thesis purpose. Attention will also be paid to describe how, in the MATLAB® script, the time subdivision into three stages (approach, turn and exit) was implemented. For both the driver models investigated, a bicycle model of the vehicle, like the one presented in Figure 2.6, was the reference vehicle model, since it was supposed to provide good results even if the complexity level was lower with respect to the other vehicle models described in the "Literature review" section (horizontal and vertical vehicle models).

3.1 Data retrieval

Since unprotected LTAP is the studied scenario in this thesis work, through video data available from EuroFOT project, it was necessary to identify suitable events. The extraction of unprotected left turns from the data was conducted manually from available recorded video, based on an initial categorisation of left turns using GPS. In order to simplify the thesis work, only "perfect" 90 degrees left turns were used in the analysis: 90 degrees left turn determination was based on video observation for each considered left turn manoeuvre. Primary analyses have been carried out on a single left turn event, a "sample" event, and then, in order to test MATLAB® code reliability, other events have been used as well.
All the suitable events was collected in an excel table; each of them characterized by different sets of parameters, which described the left turn manoeuvre. These parameters were Annotation ID, Trip ID, Driver ID, Start time, Time of 45° passage and End time of the selected manoeuvre. Few examples of collected data are represented in Table 3.1.

Table 3.1: List of some left turn events (no POV)

Annotation ID	Trip ID	Start time index [ms]	End time index [ms]	Time of 45° passage [ms]	POV type
78681	364199	124100	174100	153700	No POV
78687	331193	779000	829000	807700	No POV
78730	312929	121100	171100	143800	No POV
78743	96565	818700	868700	847300	No POV
77465	11215	192200	218900	209800	No POV
77466	65991	429300	454000	446000	No POV
77236	158833	386400	413500	403700	No POV
77302	158905	363500	389700	380700	No POV
77317	228095	616400	642700	633800	No POV

Start time and End time were measured in milliseconds; the time gap between the Start time and the End time covers the approach, turn and exit stages. The Time of 45° passage is the time when the front video shows an equal amount of the main road and the road the vehicle is turning into, as coded in the forward video. The gathered parameters were divided into two sets: the former contained trips in which drivers performed left turns at intersections with only one vehicle (POV) oncoming from ahead, the latter included left turn events in which no other road users were present at

all at or around the intersection. At a first stage of the study, no POV events were selected. Among the retrieved data belonging to each event, the GPS coordinates played an important role in order to reconstruct the SV trajectories. Dynamic parameters, such as speed, steering wheel angle and yaw rate, were collected in a vectorial form, and the sampling frequency was 10 Hz.

3.2 Study scenario

The present study scenario is made of three components: the location, the actors and the objectives. The scenario takes place at intersections, and, more precisely, at intersections where one driver is turning left without any other traffic around, as already described in the "Introduction" section. The actor is the driver, who is handling the left turn, whose relation both with vehicle and with environment is deeply analysed. The objective of this scenario consists of understanding the interaction between the driver behaviour, his/her decision making and the vehicle dynamics related to this kind of manoeuvre.

3.3 Variable selection

Once a specific 90 degrees left turn was chosen, a close look to all the collected physical variables, which characterize the event, was taken. To perform the thesis work, only some of them were really useful; these variables, listed in Table 3.2, were extracted for further implementation in both the vehicle and driver behaviour models.

Table 3.2: List of main variables for left turn analysis

Variable name	Description	Unit
Steering angle	Variable containing the steering wheel angle of the vehicle at each time step	[degrees]
Steering angle rate	Variable containing the steering wheel angle rate of the vehicle at each time step	[degrees/s]
Vehicle speed	Variable containing the speed information of the vehicle at each time step	[m/s]
Yaw rate	Variable containing the yaw rate information of the vehicle at each time step	[degrees/s]
Time index	Variable storing the time elapsed since the beginning of the trip	[ms]
GPS position	Variable containing the GPS coordinates of the vehicle at each time step	[m]
Lateral acceleration	Variable containing lateral acceleration of the vehicle at each time step	[m/s^2]
Longitudinal acceleration	Variable containing longitudinal acceleration of the vehicle at each time step	[m/s2]
Distance travelled	Variable storing the distance travelled since the beginning of the trip	[m]

3.4 Data overview

For a better understanding of the raw variables, MATLAB® was used to generate plots in order to get a better idea of the measured parameters values. As depicted in Figure 3.1, the vehicle trajectory of the trip chosen as sample (Trip ID: 11215) for the entire thesis work was plotted; the red circle points out the exact left turn event analysed, which corresponds to a perfect 90 degrees left turn across path with no POV, as stated before. Throughout the entire Method chapter, all the figures will refer to such trip; evaluation of driver parameters, like the desired longitudinal acceleration, from other left turn events will be collected and properly explained in the "Results" section. In addition, real driving data regarding the steering wheel angle rate and the steering wheel angle are shown, respectively, in Figures 3.2 and 3.3.

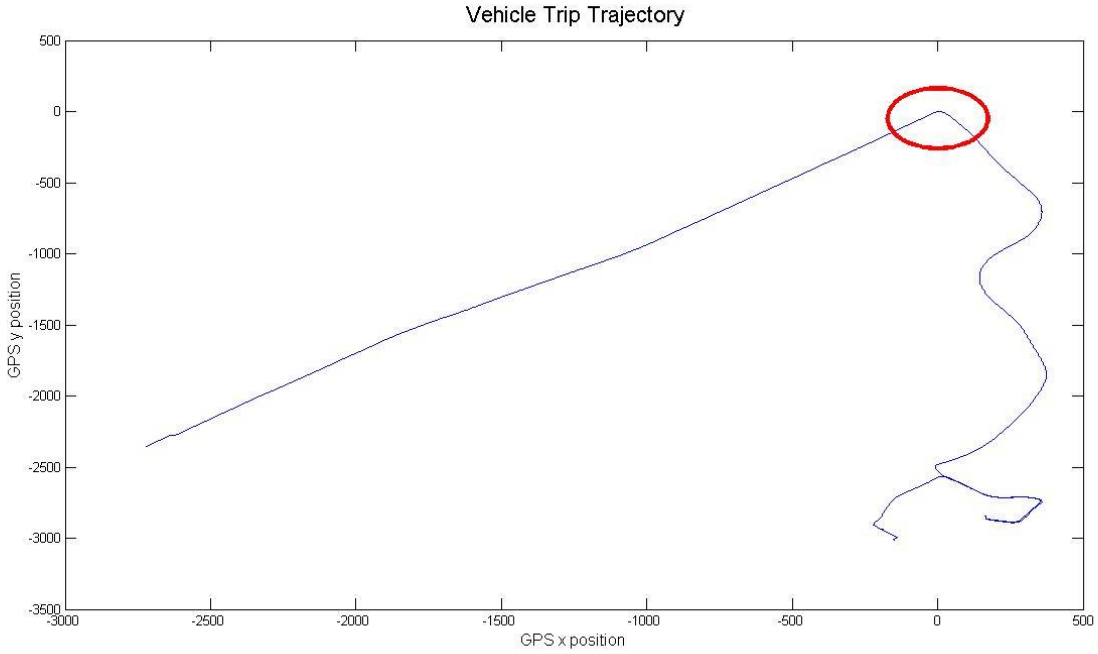

Figure 3.1: Vehicle GPS trajectory for sample trip (Trip ID: 11215) with indication of left turn event

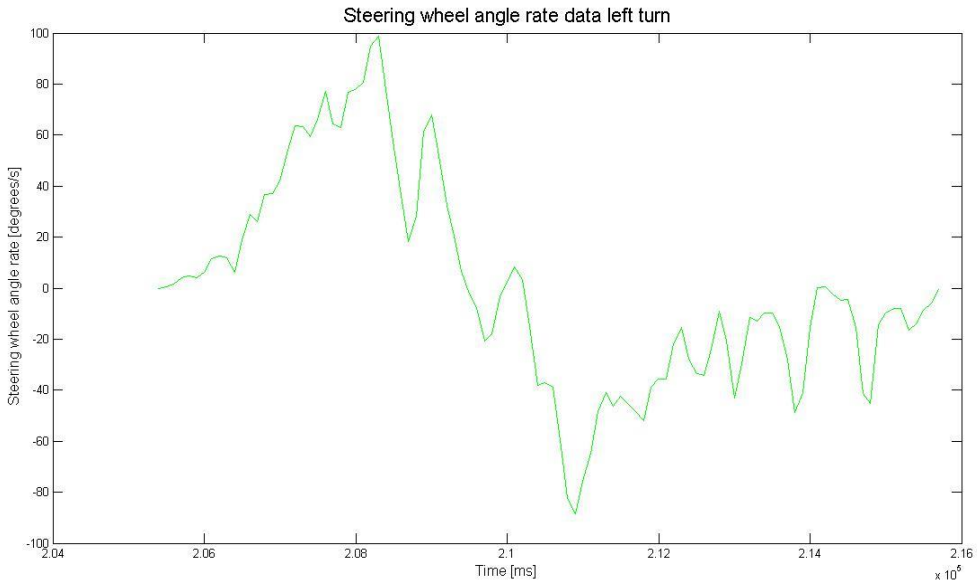

Figure 3.2: Steering wheel angle rate for sample trip (Trip ID: 11215) during left turn event

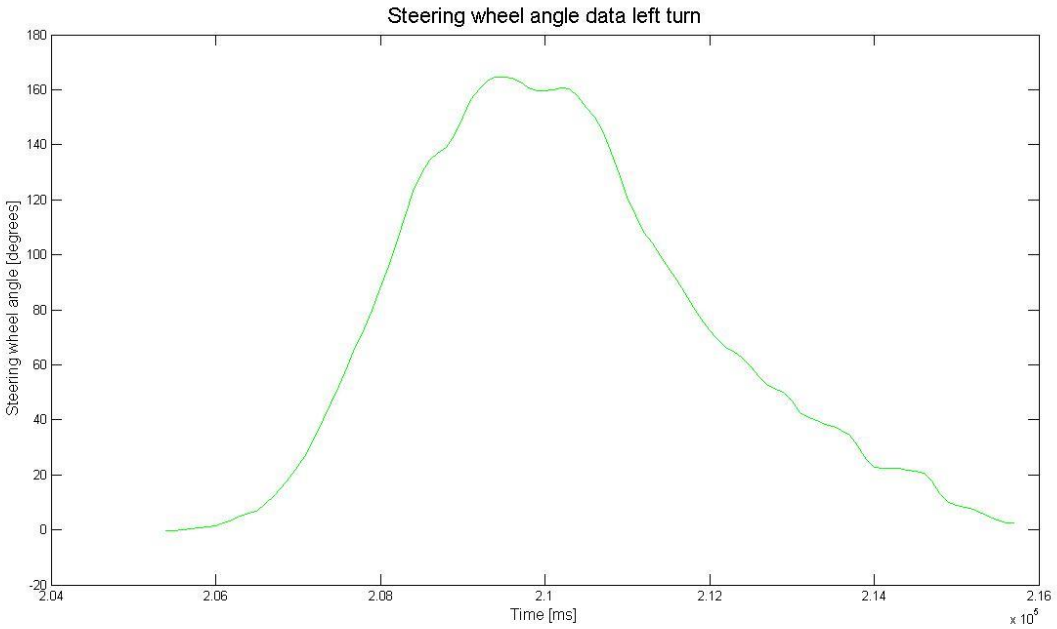

Figure 3.3: Steering wheel angle for sample trip (Trip ID: 11215) during left turn event

3.5 Left turn delimitation and trajectory reconstruction

The first aim of the work, once the main useful variables were identified, consisted of setting the time boundaries among the three stages: approach, turn and exit. In the Salvucci and Gray's model the thesis work only dealt with the turning stage; it was therefore important to move backward and forward with respect to the "Time of 45° passage", in order only to include the most interesting stage; running the simulation from the Start time to the End time, indeed, would have been useless, as it would have contained all the three stages of a left turn manoeuvre. A script was prepared in MATLAB® to consider driving data from the left turn only once a certain steering wheel angle had been reached. A steering wheel angle of 8 degrees had been chosen

to divide the approach stage from the turn stage, because, after few trials, it was discovered that it was a good compromise between two opposite trends: if the steering wheel angle is too low, the MATLAB® code begins extracting data well before the turn stage starts; on the other hand, high values of steering wheel angle are reached once the turning stage has already started, and this would lead to a significant loss of important data.
Once reached the first threshold for the steering wheel angle, the MATLAB® script kept on saving vehicle data until another predetermined steering wheel angle has been encountered. For the same reason explained before, it was found that a good time threshold between turning and exit stage could have been established when a steering wheel angle of 2 degrees was reached. In this way it was feasible to filter available data without losing important information about the turning stage.

3.6 Salvucci and Gray's model: evaluation of driver behaviour

After having evaluated the period of time covered by the turning stage, an analysis on driver behaviour and other dynamics parameters according to Salvucci and Gray theory has been conducted.
During the approach stage the driver is assumed to look and use the near and far points as described in Salvucci and Gray (2004), but when the turning stage starts a new position of the near and far point is defined. This switching point becomes a very important moment that is very difficult to model as there is no study that exactly states when this action takes place, then remaining unknown, and the driver switches the gaze point unconsciously. Regarding the turning stage, it was decided to position the near and far points in the exit road and only move on the *x-axis* direction (Figures 3.4 and 3.5). The new positions of the near point "n" and the far point "f" stand in the middle of the lane the driver is aiming to enter, at a certain distance from the *y-axis*, being the far point always further than the near point. In other words, at the beginning of the turning stage both near and far points are close together or even at the same location and change over time with the position of the car.

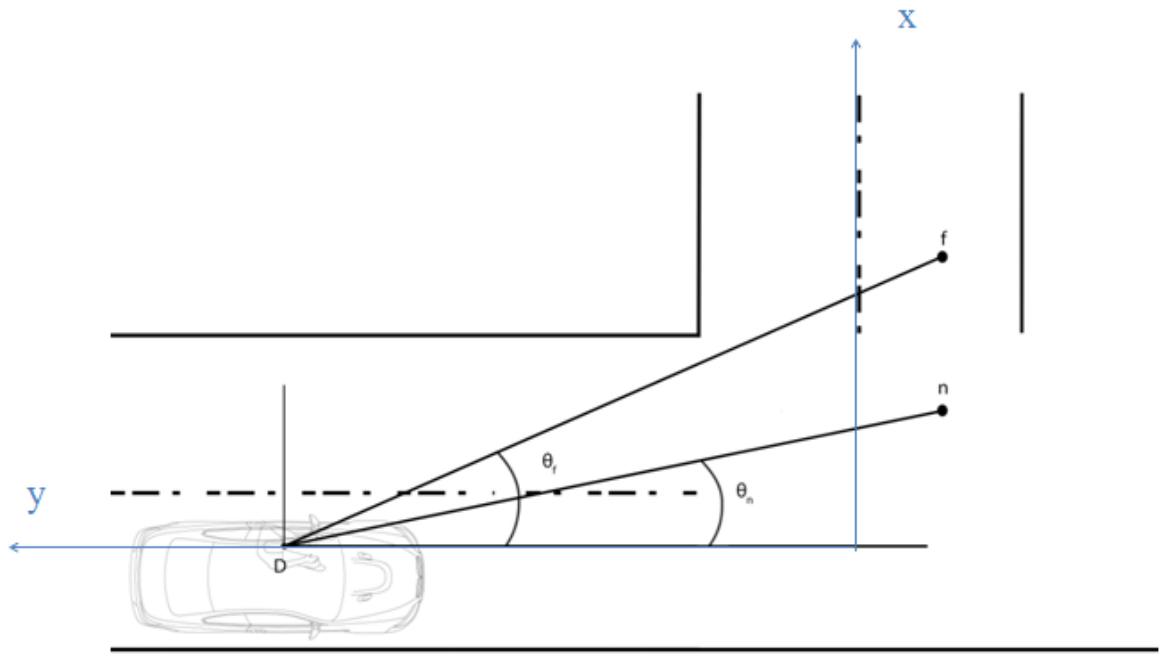

Figure 3.4: Generic near and far point position at the beginning of the left turn. "n" and "f" in the figure correspond to the near and far points location, θ_n and θ_f their respective angles and "d" the driver position.

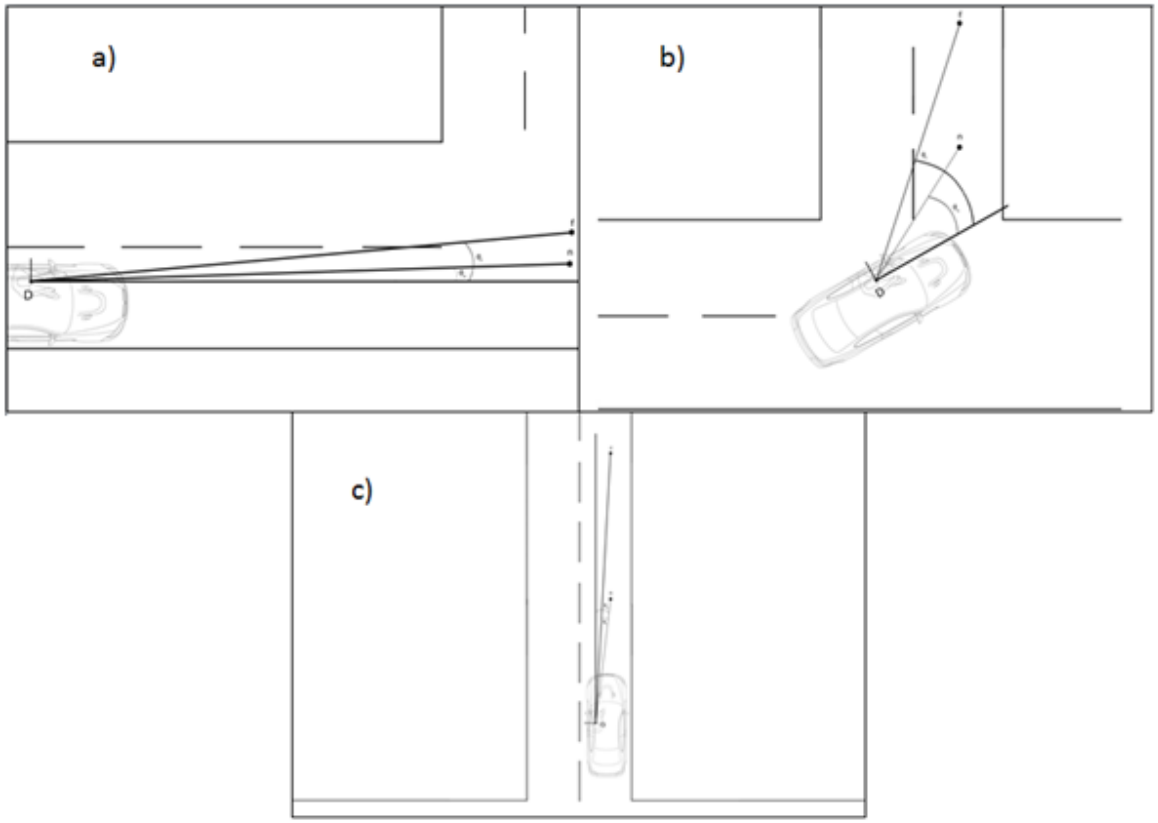

Figure 3.5: New near and far along the left turn: a) approach stage, b) turning stage, c) exit stage

Furthermore, d_n and d_f evaluation can be made, based on the following system of equations:

$$\begin{cases} d_n = k_s \cdot \left| delta_y \right| + d_{n_{\min}} \\ d_f = d_n + dfdelta \cdot x \end{cases} \tag{3.1}$$

Table 3.3: Near and far points parameter definition

Variable	Description
d_n	near point distance
d_n_min	minimun near point distance
k_s	near point proportional coefficient
delta_y	distance traveled by the car on the y-axis
d_f	far point distance
X	x-axis position of the car
Dfdelta	far point proportional coefficient

As regards parameters collected in Table 3.3, *d_n* corresponds to the distance on the *x-axis* of the near point, as seen in the system equation (3.1); its value increases alongside the distance between the car and the intersection, *delta_y*. *k_s* represents the coefficient in charge of controlling the variation of *d_n*, starting from its minimal distance *d_n_min*, calculated by the genetic algorithm in order to obtain the optimal proportional ratio during the left turn. On the other hand, *d_n* and *x*, the near point distance and the position of the car on the *x-axis* respectively, are the two variables needed to calculate the position of the far point *d_f*; hence the far point distance increases constantly together with the distance from the car to the *y-axis*, *x*. (see Figure 3.5)
The coordinates system was located in a way in which the x-axis would correspond to the centre line (dash-dotted vertical line in Figure 3.4) of the exit road and the y-axis would be located in the approach road at the position of the passenger to be as close as possible with the existing model (see Figure 3.4).

3.6.1 Evaluation of driver behaviour model

Previous research and particularly previous work from Benderius, on Salvucci and Gray's model, established a starting point for this thesis as the basic code, describing the model and the car variables, was provided for its implementation. This initial code, composed of 3 main MATLAB® files (car dynamics, driver model and the code for running it), previously adapted by Benderius for his specific scenario mentioned in the literature part, was analysed. The decision made, after getting the code, was to implement it for a specific driver, a specific trip and a specific event (LTAP/OD). In particular, the same trip used in the Nobukawa's model implementation was chosen. Then the second step was to scale the model up using different events from the same driver. Finally a larger number of drivers and events would have been analyzed with the model and its performance and accuracy would have been evaluated. In this thesis only the first step was carried out. The initial trials were conducted directly with the provided code and then a new one was built since a new approach was necessary given that the conditions were different. The car dynamics and the equations to

calculate them were re-evaluated and made suitable for the geometry of the new scenario with new initial conditions and parameters. The MATLAB® code used is composed of the following files that enable the model to calculate the parameters and run the simulation:

- dataAnalysis: file that extract the input data from the database and saves it for its further use;
- realDataGA: file where the input data is loaded, the initial conditions set and that is in charge of running the whole model;
- realDataGAWrapper: file that runs the genetic algorithm and generates the parameters.
- realDataDM: file containing the driver model implementation;
- stepLinearVehicle: file containing the equations for calculating the position, speed and heading angle of the car;
- Optimplot: file that contains the complementary code to observe the GA generation process if wanted (not crucial for the model).

Loading the required data is the first thing the code does when running it and after the options for the Genetic Algorithm (GA) are established the GA iteration process starts. The best parameters are then calculated and extracted from it for finally being used as inputs variables for the driver model. Subsequently last outputs plots and parameters values are finally obtained and plotted for their further analysis (see Figure 3.6).

Figure 3.6: MATLAB® files process flow chart

Note that the initial conditions set for the model are the ones extracted from the real data, while the others are calculated by the model itself. Concerning them, for the new situation the car heading angle was considered to be 90 degrees, as it is the angle between the approach road and the exit road, and the initial offset position of the car when the tuning stage started was set at 44 meters, corresponding to the initial distance between the vehicle and the intersection when the left turn starts. This distance was evaluated from the trip data analysis previously performed. The option of using the real data at each time step was envisaged but as the model was required to work independently the decision of letting the program feed itself was chosen.

3.6.2 Genetic algorithm and cost value functions

Two optimization functions incorporated in MATLAB® are fminsearch and the GA. For this thesis work the GA was the option chosen for the optimization as it suited best the requirements needed. The main utility of the mentioned function is to generate a population of optimized parameters, specified by the user, in order to

obtain the minimum error and solve the optimization problem. For that purpose, a population of points, at each iteration, is generated and evaluated by the GA; different options are available for the user, allowing him the possibility to set constraints to this generation and decide the population size and generation size among others. At the end the best parameters generated are saved as a variable. Another important factor to take into account when using the genetic algorithm is the cost value function, which is the function that the GA will minimize at each iteration in order to obtain the best parameters for the optimization. It has to be defined properly to minimize the error as the output could be highly affected by it and thus having a good cost value function is essential. Different outputs are obtained every time the program files are executed as the parameter generation of the GA varies every time hence the simulation could differ one from another depending on this generation. Seven parameters were chosen to be generated and optimized by the GA (parameters detailed description is included in the Results section) letting a high level of freedom to the model. Furthermore, the only constraints imposed to the GA were the initially set up of the number of iterations, that corresponded to 1000, the cost value function and finally the boundaries of each parameter (also described in Results section).

3.6.3 GA parameters and cost function evaluation

The GA was added and was in charge of obtaining the best values for the coefficients in the respective driver models. For the Salvucci and Gray's model, initially seven parameters where chosen to be evaluated and optimized by the genetic algorithm: the three coefficients of the Salvucci and Gray's model (k_n, k_f, k_I), the near and far points coefficients (*k_s*, *dfdelta*), the car steering wheel relation (G) and the cost value function coefficient (x(7)) and alongside those parameters their boundaries were defined as constraints inside the options of the GA, as it is shown in Table 3.4.

Table 3.4: The seven parameters optimized by the GA function and their relative boundaries

Parameter	Boundaries [lower boundary, upper boundary]
Kn	[0,30]
Kf	[-3,30]
Ki	[-3,30]
G	[15,25]
Ks	[0,1]
Dfdelta	[0,2]
X(7)	[0,1]

The cost function below was the one used by the model to minimize the error:

$$\cos tvalue\_swar = \sqrt{\sum\left(k_f \cdot \dot{\theta}_f + k_n \cdot \dot{\theta}_n + k_I \cdot \theta_n - swar \cdot \frac{\pi}{180}\right)^2} \qquad (3.2)$$

$$\cos tvalue\_swa = \sqrt{\left(\int\left(k_f \cdot \dot{\theta}_f + k_n \cdot \dot{\theta}_n + k_I \cdot \theta_n\right) - \int\left(swar \cdot \frac{\pi}{180}\right)\right)^2} \qquad (3.3)$$

$$\cos tvalue = \cos tvalue\_swar \cdot (1 - x(7)) + \cos tvalue\_swa \cdot x(7) \qquad (3.4)$$

This cost value function implies the intention of obtaining optimal parameters minimizing both the calculated steering wheel angle rate (swar) and the steering wheel angle (swa) errors at the same time. The x(7) was only used to evaluate the appropriateness of including both the steering wheel angle rate (swar) and the steering wheel angle (swa), and not only the swa cost value.

3.6.4 Output plots and results

The final step consisted on checking the optimization and the new code well-functioning. For that purpose, every time the model was executed, plots where generated and then compared. Plots of the desired variables calculated by the model such as the steering wheel angle rate and the steering wheel angle were plotted alongside the real data of the event and then checked to confirm that the code was achieving properly what was expected. Error functions to have a complementary visual output of the level of fit obtained where also included subsequently. Finally, in addition to those plots, secondary plots showing the near and far point distances evolution, the heading angle of the vehicle and the left turn trajectory were added to help detect errors when the output was not the desired one and to monitor the effect of the GA generated parameters on the final result.

3.7 Nobukawa's model: evaluation of speed and acceleration profiles

Once a real vehicle trajectory had been defined and target point Q (refer to Figure 2.15) had been set at the end of the turning stage, it was possible, at each time step, to calculate the length of the distance *d* between the actual vehicle position and the target point Q. Similarly, setting the heading angle at Q equal to 90 degrees, it was possible to evaluate the change in heading angle $\Delta\psi$ at each time interval by simply making the difference between the heading angle at the current vehicle position (easy to get from GPS position) and the heading angle in Q. By using the equations (2.29) and (2.30), already discussed in the "Literature review" section (Paragraph 2.2.2), the value of the "hat" lateral acceleration $\hat{a}_y$, the "hat" longitudinal acceleration $\hat{a}_x$ and the curvature radius *R* have been defined. It is reasonable to expect that all these values change with time, since the distance *d* is defined by Nobukawa et al. (2012) as the segment which links the target point of the turning stage (fixed) with the actual vehicle position point (not-fixed) and all other values depend on *d* itself. Figure 3.7 shows the behaviour of the two "hat" accelerations during the turning stage, compared with the measured longitudinal and lateral accelerations, respectively a_x and a_y.

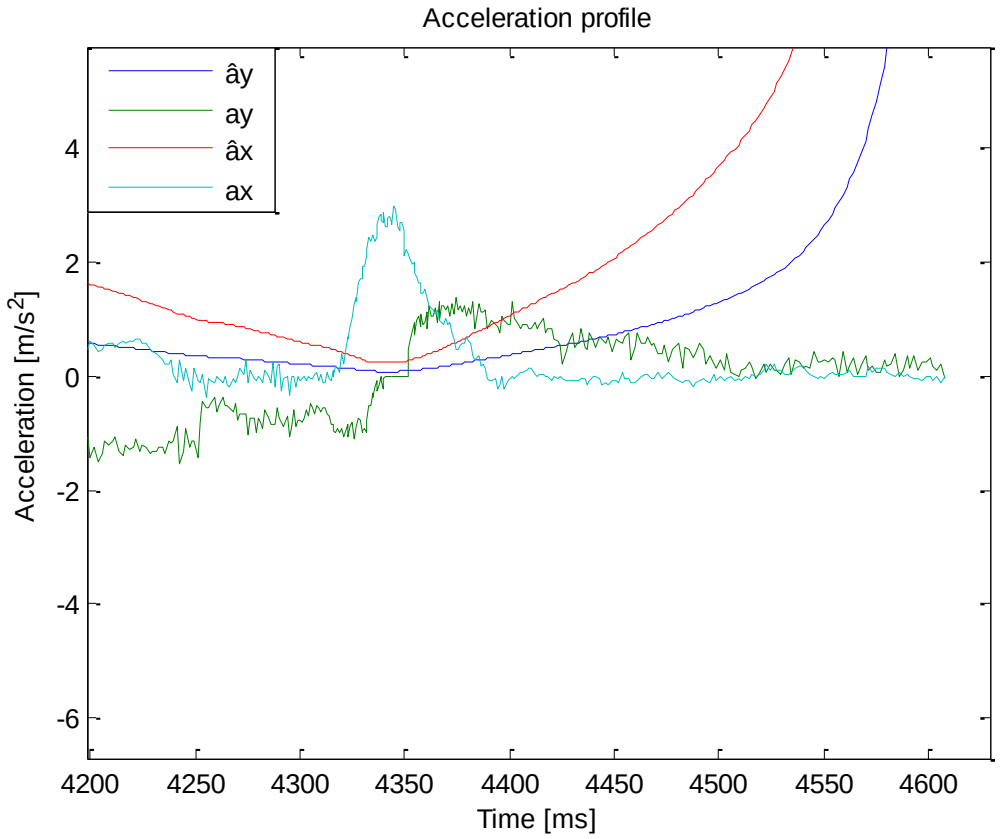

Figure 3.7: Measured and anticipated accelerations (both lateral and longitudinal) (Trip ID:11215)

Once vehicle parameters have been stated, an initial value for driver parameters for left turn has been manually provided in order to start the genetic algorithm optimization; initial values, close to the final ones found by Nobukawa et al. (2012) in order not to alter too much final results, are collected in Table 3.5. Boundary conditions have been fixed to driver parameters for the genetic algorithm in order to obtain reasonable values parameters.

Table 3.5: Initial driver parameter values

Symbol	Quantity	Initial value
K [Hz]	Proportional gain	2
lb_2 [m/s^2]	Lower bound of desired $\hat{a}_y$ range	2
a_2 [m/s^2]	Saturation value for turn stage	0.5
ub_2 [m/s^2]	Upper bound of desired $\hat{a}_y$ range	3

In this specific case, for the genetic algorithm, the optimization objective consists of having a speed model profile as close as possible to the measured speed, as evidenced in Figure 3.8. In order to work, the genetic algorithm requires a cost value function, that has to be minimized in an optimization problem. A cost value function, given by the difference between the speed of the model and the measured speed at each time step, has been used.

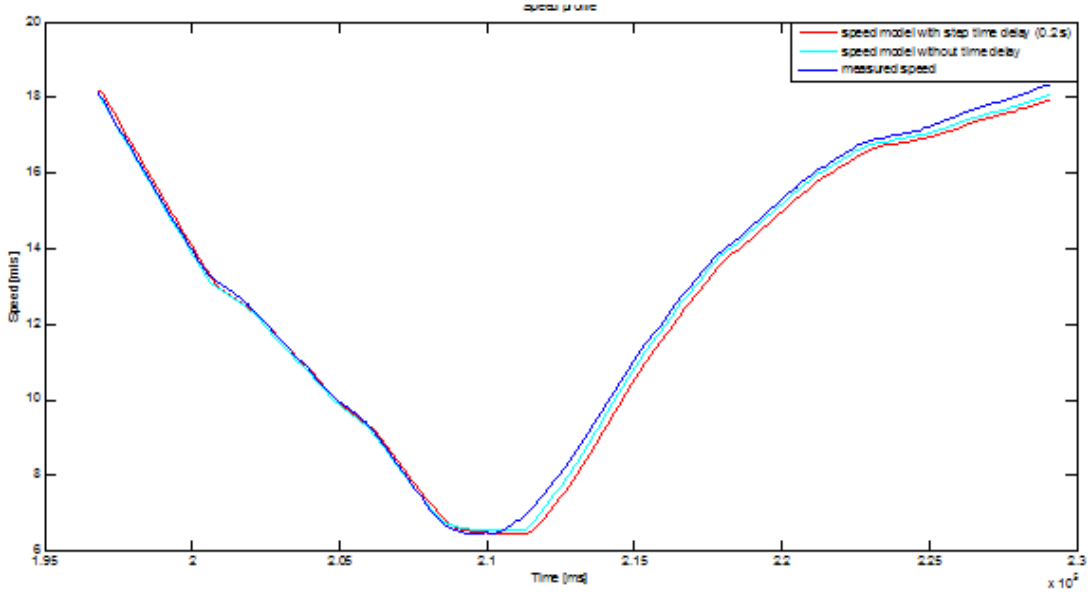

Figure 3.8: Speed model compared to measured vehicle speed (Trip ID: 11215)

The knowledge, over time, of the values of the anticipated acceleration reference and of the speed model were then used to obtain, through a step-wise linear function like the one highlighted in Figure 2.16b, the curvature of the desired longitudinal acceleration. From the optimization, the parameters K, lb_2, a_2 and ub_2 were obtained and the desired longitudinal acceleration was computed and plotted, following the instructions given by Nobukawa et al. (2012) for the turning stage. This desired longitudinal acceleration has been compared to the real one and their difference (error) was calculated. Figure 3.9 represents the desired longitudinal acceleration for the sample trip taken into account, while Figure 3.10 shows the comparison between the two accelerations (desired and measured) and the generated error, which is perceived by the driver, who acts on the gas or brake pedal if, respectively, a_x^{des} is higher or lower than measured a_x.

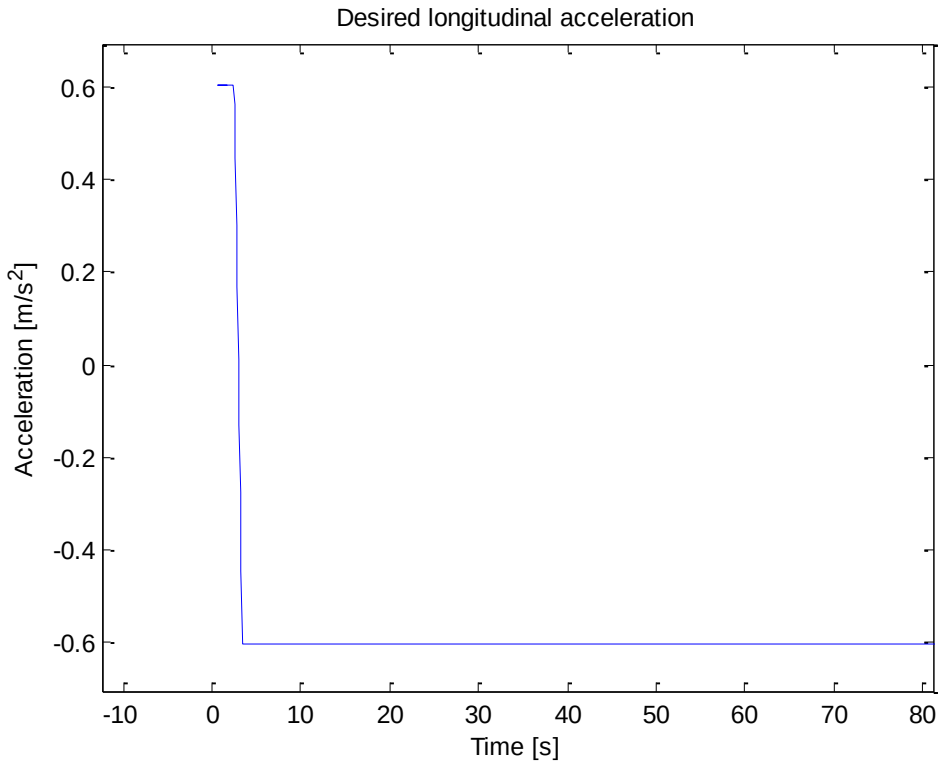

Figure 3.9: Desired longitudinal acceleration (Trip ID: 11215)

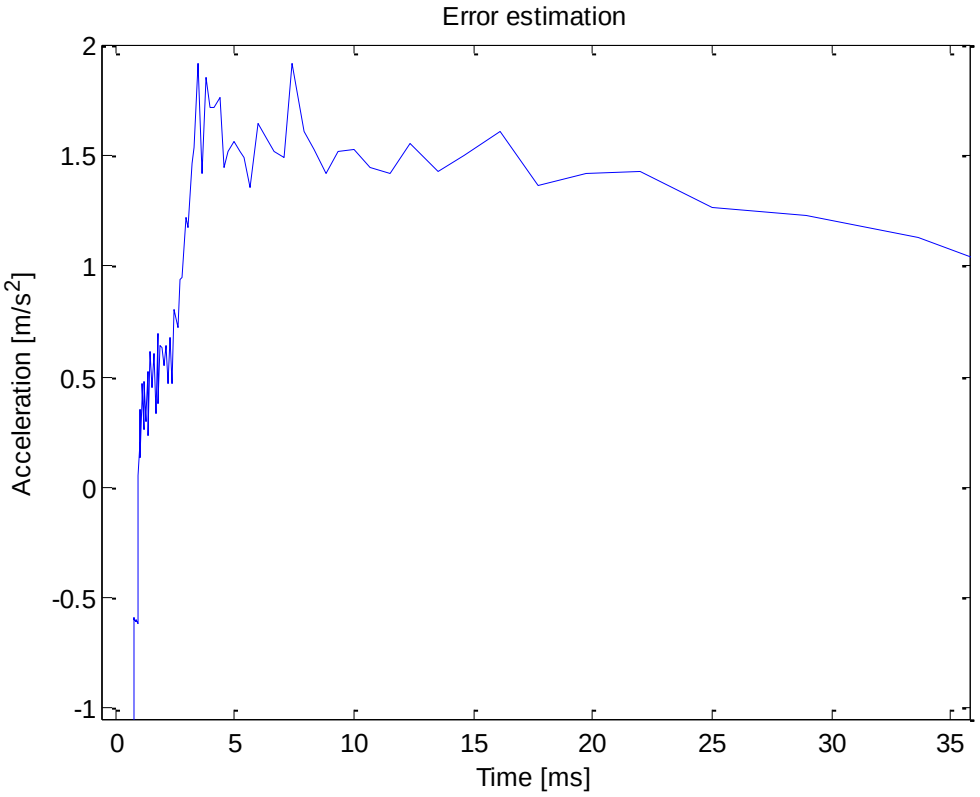

Figure 3.10: Error estimation (Trip ID: 11215)

Once the speed model has been computed and the analysis of the longitudinal and lateral accelerations has been performed, reliability tests have been sustained considering three new intersections dealt by the same driver. The simulation results are shown in the "Results" section.
Starting from the plot in Figure 3.8, it was manifest that a high fitness level had been reached between measured speed and speed model for the considered left turn. A deeper analysis, therefore, was conducted to investigate if the simulation also provided an appropriate fitness between measured speed and speed model in other types of left turn events. It was therefore chosen to find left turn events similar to the one investigated above through the use of SQL Developer. Other intersections, always dealt by the same driver, were found and, among them, a new one was chosen as a new case to analyse. The GPS trajectory of the vehicle in the considered intersection is reported in Figure 3.11, whereas the relationship between the measured speed and the speed obtained from the model is shown in Figure 3.12.

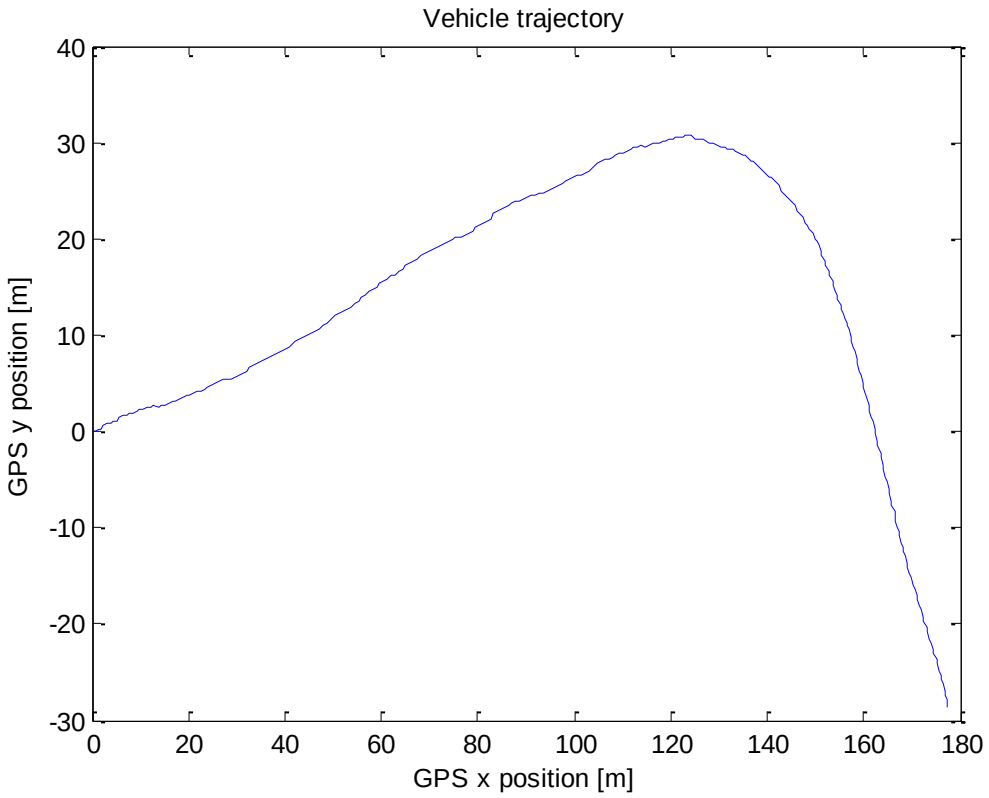

Figure 3.11: Vehicle trajectory for a second left turn intersection

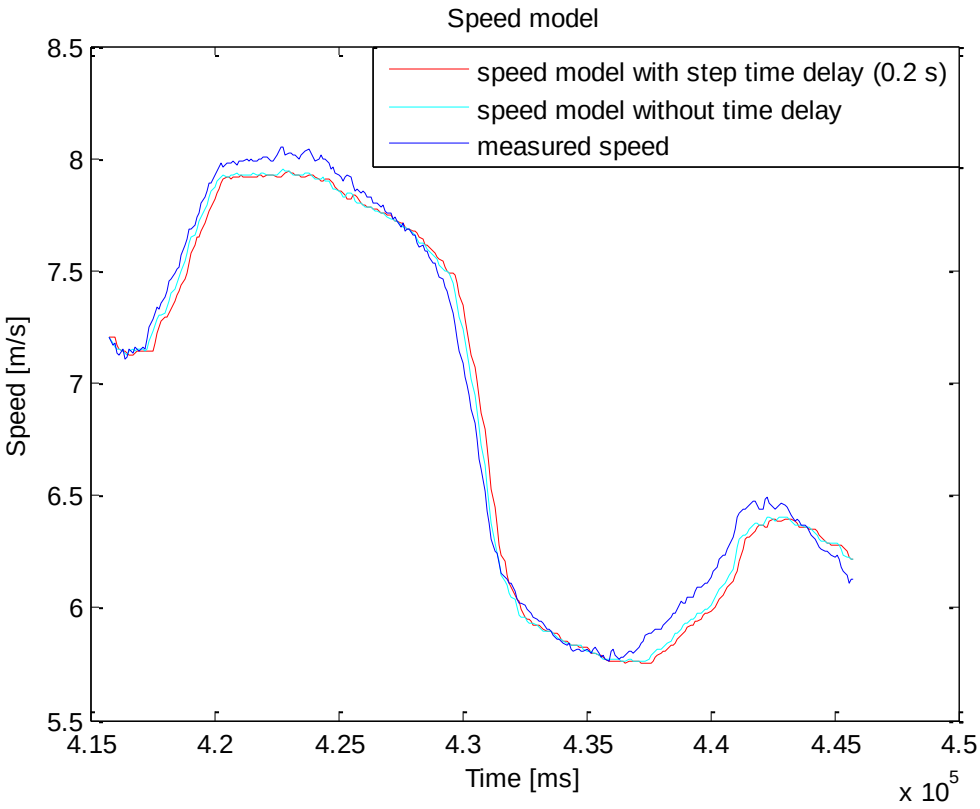

Figure 3.12: Speed model for a second left turn intersection

4 Results

4.1 Salvucci and Gray's model

After running the model several times, an anomaly was observed: The steering wheel angle value at the end of the turn was negative, the left turn performed by the driver was not a perfect 90º left turn and the heading angle at the end of the manoeuvre was positive; values that did not represented the reality of the event. Further analysis was performed to understand the effect of the cost function parameter x(7), and thus the cost function itself, in the output of the model. The analysis consisted of executing a MATLAB® script 20 times and after each run, the parameter value was extracted into an excel file and sorted out based on a visual observation of the values obtained of all the different outputs. The objective of this analysis was twofold:

1) to find out what values of x(7) conducted to the an undesired output and which ones allowed the best optimization results;
2) to observe if any of the other parameter converged to a constant value, so that it could be replaced or even removed from the GA, simplifying the code.

The main result of this analysis was that bad fitting results were obtained when the cost value parameter value, corresponding to x(7) in equation 3.4, was equal to 1, which means that the cost function used for the optimisation only minimized the steering wheel angle and not the steering wheel angle rate, and the opposite results when it was close to 0.
Considering that the output obtained was not regularly satisfactory, the cost function reported in equation 3.4, which combines the errors of the steering wheel angle rate and the steering wheel angle (measured and calculated), was changed. A new cost value function was considered only minimizing the error between the steering wheel angle rate measured and the one calculated. This new cost function was derived from the previous one, setting the parameter x(7) equal to 0:

$$\cos tvalue = \cos tvalue\_swar \tag{4.1}$$

The new cost function allowed to obtain stable results every time the code was executed.

4.1.1 List and description of results

The results described in this section are divided into four parts:

- steering wheel angle rate;
- steering wheel angle;
- vehicle heading angle;
- left turn trajectory.

Steering wheel angle rate: Real data, driver model and error

Figure 4.1 shows the steering wheel angle rate from the real data and the one calculated by the driver model, blue and red lines in the figure respectively. As well, the error between the real data and the model at each point is shown in green in Figure 4.1. Constant corrections of the steering wheel angle by the driver, observed in the real data, shape the aspect of the steering wheel angle rate and of the error, explaining the sudden peaks. Overall, the model follows quite accurately the shape of the real data excluding the beginning of it, in which we can notice an initial error of about 20 degree/s. This difference between the measured and real steering wheel angle rate is probably due to the switch from the approach stage to the turn stage: during this switch, the near and far point positions change instantly and the model seems not to adapt as fast as human does. The r-squared error obtained for the steering wheel angle rate, in this case, is 0.8509 which is a good indicator that the fit is good.

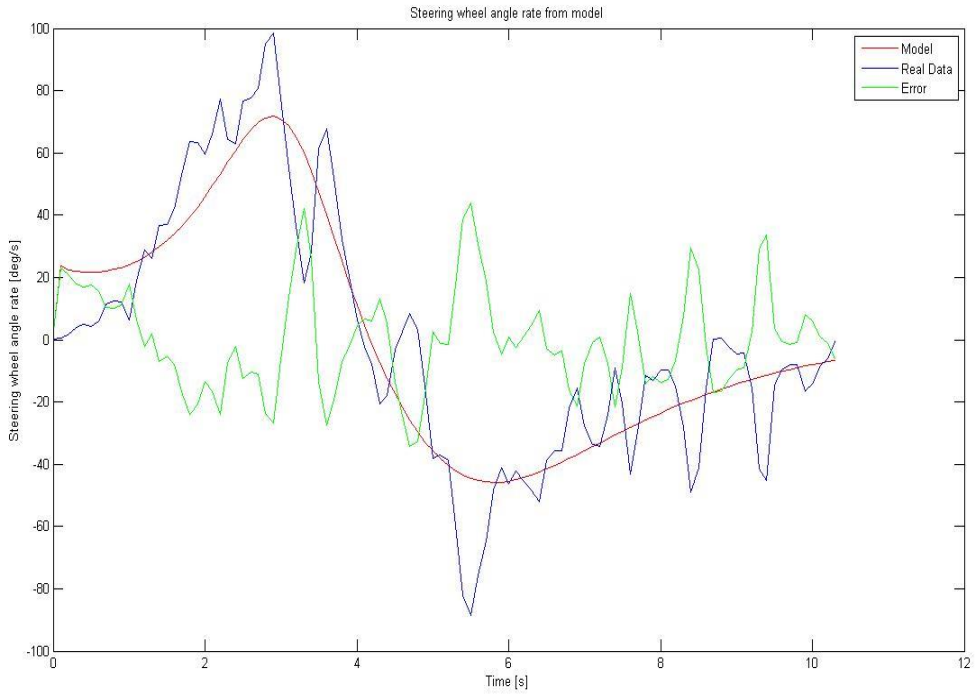

Figure 4.1: Steering wheel angle rate (real data, driver model and error)

Steering wheel angle: Real data and driver model

Figure 4.2 shows the steering wheel angle corresponding to the real data (blue line) and the steering wheel angle calculated by the model (red line). The error is drawn in green in the same figure and, in this case, it fluctuates between 18 degrees and -11 degrees approximately. The model describes the real data quite well as we can see in the figure supported by the r-square value which is 0.9839. In addition to that as in the chart of the steering wheel angle rate, there is an initial error due to the switch from the approach stage to the turn stage.

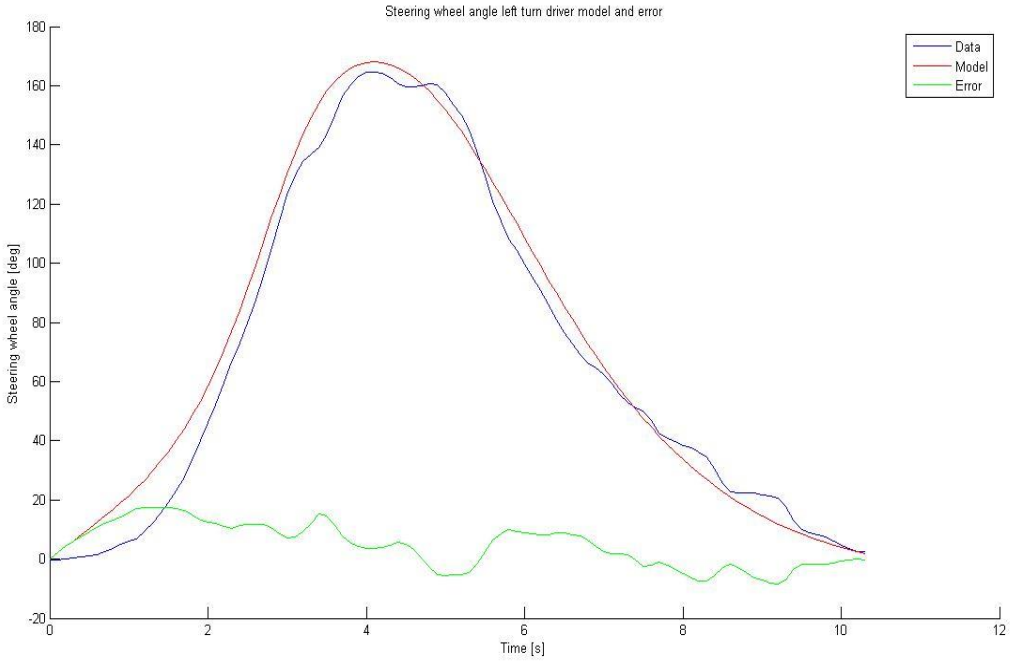

Figure 4.2: Steering wheel angle (real data, driver model and error)

Vehicle heading angle

As shown in figure 4.3 the car initial heading angle matches perfectly to -90 degrees corresponding to the initial conditions setup of the left turn, established as the initial condition due to the new coordinate system definition. Through the course of the turn the modelled vehicle heading angle evolves until he reaches 0 degrees approximately which indicates that the car is going straight on the exit road as it happens during the real event.

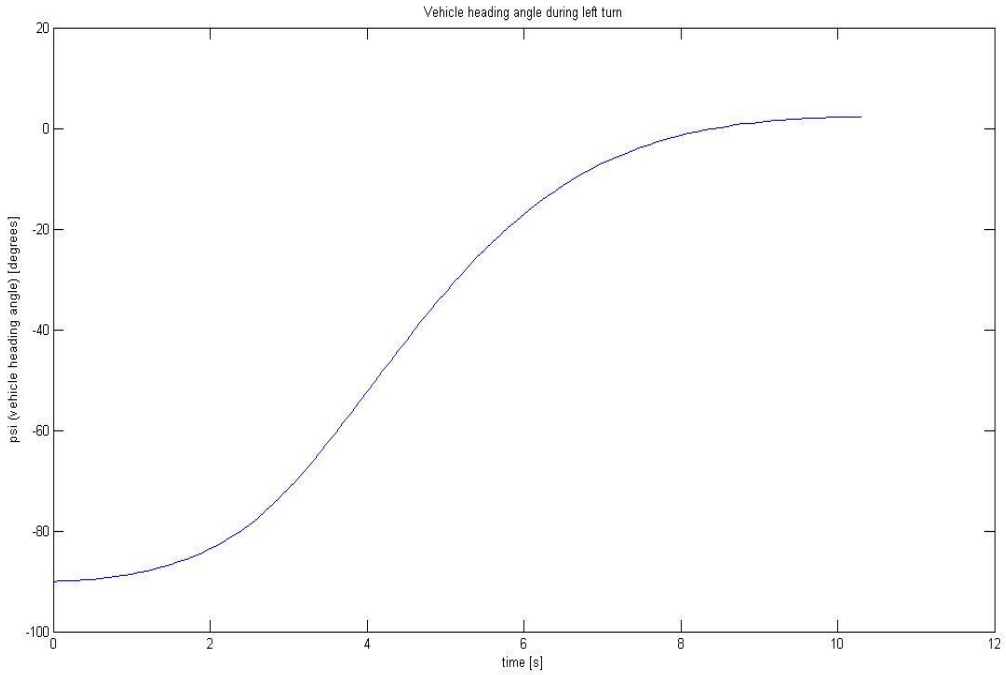

Figure 4.3: Heading angle

Left turn trajectory from model

Figure 4.4 shows the trajectory described by the SV, during the left turn, obtained with the model. Starting at the initial position of 44 meters on the y-axis, the model describes an almost perfect arc, similar to the real data, and the turn ends with the car heading straight on the exit road.

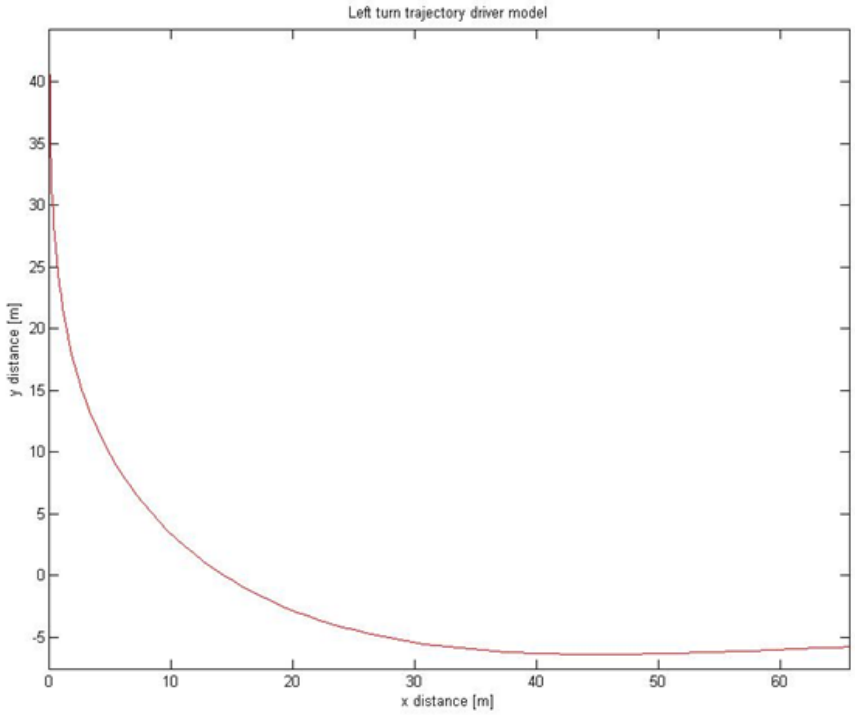

Figure 4.4: Left turn trajectory from model

Near and far points distance

Figure 4.5 shows the evolution of the distance of the near and far points from the SV on the exit road during the left turn. As the SV proceeds in the turning stage, both distances increase. Starting from the minimum distance (5 meters) the near point reaches a distance close to 15 meters in front of the car. The far point, located in the same position as the near point in the beginning of the turning stage, reaches a distance of about 350 meters, which is a reasonable distance considering no POV presence.

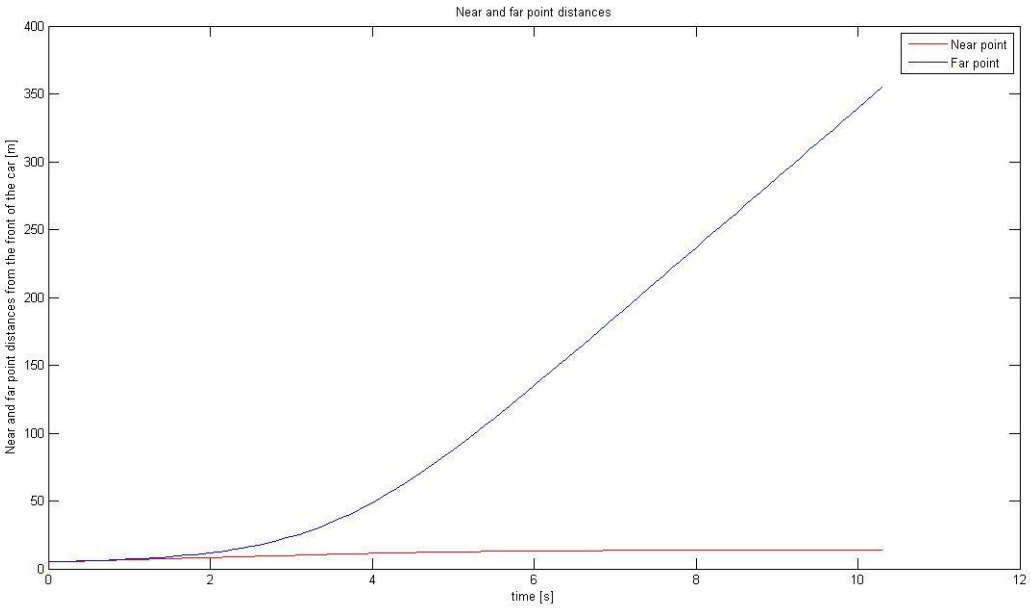

Figure 4.5: Near and far points distances from the subject vehicle

The GA optimised parameters values, obtained during this specific simulation, are collected in Table 4.2. These parameters correspond to the ones utilised, when generating the previous plots, as the final input when executing the driver model for the last time.

Table 4.2: GA optimization parameters value

Parameter	k_I	k_n	k_f	G	k_s	*dfdelta*
Value	0.0136	2.9529	3.5002	24.3647	0.1700	5.2894

4.2 Nobukawa's model

Once the model had been optimized for two trajectories (two left turn events) with respect to the speed profile, more attention was paid to the reproducibility of driver parameter values created by different runs of the genetic algorithm in order to fit the speed model to the real speed profile. For each of the two left turn events considered so far, two different factors could be varied: the number of driver parameters evaluated by the genetic algorithm and the lower and upper boundaries limits of the driver parameters. As regards the former factor, it was chosen to evaluate one solution

with three parameters (optimization of lb_2, a_2 and K, while ub_2 is fixed equal to lb_2+1) and one solution with four parameters (optimization of lb_2, a_2, K and ub_2). The benefit of having a reduced number of parameters to optimize by the genetic algorithm consists of having a less time-consuming simulation; moreover, too many parameters can result in an over-fit of the model, not supporting any generalization. It is however also important to consider that a too small number of parameters could give worse results for the fitting. Similar could be done for the latter factor (boundaries for the parameters), which allowed to set the lower and upper boundaries by increasing or decreasing the gap between them. A "narrow" manipulation supports model generalization and it is characterized by a smaller gap between lower and upper boundaries: this condition leads to increased speed to run the simulation, and also higher risk not to include the optimal value within the two boundaries for the parameter (and, therefore, higher risk not to have a close fit between model and measurements). Opposite reasoning is valid for the "expanded" manipulation. The Table 4.3 shows the setting of the lower and upper boundaries used in the simulation, after taking into account results obtained by Nobukawa in his previous works.

Table 4.3: Genetic algorithm boundaries for each parameter and manipulation type

Manipulation	Boundary conditions	K	Lb_2	a_2	ub_2
"Narrow" manipulation	Lower boundary	0	0	0	2
	Upper boundary	4	2	3	6
"Expanded" manipulation	Lower boundary	0	0	0	3
	Upper boundary	6	3	4	6

Since two different states are present for each varying factor, four combinations can be obtained (three parameters-narrow manipulation; three parameters-expanded manipulation; four parameters-narrow manipulation; four parameters-expanded manipulation).
For both the events considered in this thesis, the simulation has been run 5 times for each combination. The root mean square errors of both the speed (*RMSE_speed*) and the longitudinal acceleration (*RMSE_ax*) profiles were also calculated: results are collected in Tables 4.4 – 4.11. Tables 4.4 - 4.7 refer to the first left turn event (the one analysed in the "Method" chapter), while Tables 4.8 - 4.11 are related to the second left turn event (described at the beginning of this paragraph).

Table 4.4: Genetic algorithm optimization in "narrow" manipulation, ub_2 fixed ($ub_2=lb_2+1$) – first left turn

N° trials	K	lb_2	a_2	ub_2	*RMSE_speed*	*RMSE_ax*
Trial 1	1.1074	1.2737	0.0155		0.8306	0.6770
Trial 2	1.0810	0.1276	0.0170		0.8316	0.6857
Trial 3	1.0906	0.3200	0.0111		0.8314	0.6822
Trial 4	1.0755	0.0437	0.0168		0.8319	0.6862
Trial 5	1.0990	0.6899	0.0145		0.8311	0.6801
Mean	1.0907	0.4910	0.0150		0.8313	0.6822
Std. deviation	0.0130	0.5034	0.0024		0.0005	0.0039

Table 4.5: Genetic algorithm optimization in "expanded" manipulation, ub_2 fixed ($ub_2=lb_2+1$) – first left turn

N° trials	*K*	lb_2	a_2	ub_2	*RMSE_speed*	*RMSE_ax*
Trial 1	1.1059	1.1177	0.0136		0.8307	0.6778
Trial 2	1.1145	1.4788	0.0171		0.8308	0.6759
Trial 3	1.0796	0.0953	0.0171		0.8317	0.6859
Trial 4	1.0732	0.0250	0.0195		0.8319	0.6875
Trial 5	1.0789	0.0880	0.0178		0.8317	0.6863
Mean	1.0904	0.5610	0.0170		0.8314	0.6827
Std. deviation	0.0185	0.6856	0.0021		0.0006	0.0054

Table 4.6: Genetic algorithm optimization in "narrow" manipulation, ub_2 not fixed ($ub_2=x(4)$) – first left turn

N° trials	*K*	lb_2	a_2	ub_2	*RMSE_speed*	*RMSE_ax*
Trial 1	1.0987	0.5431	0.0136	2.2951	0.8309	0.6792
Trial 2	1.0962	0.0980	0.0151	2.5053	0.8309	0.6804
Trial 3	1.1389	0.5143	0.0311	5.2764	0.8350	0.6722
Trial 4	1.1958	1.9955	0.0472	5.6286	0.8490	0.6624
Trial 5	1.1383	0.0040	0.0435	4.3077	0.8403	0.6756
Mean	1.1336	0.6310	0.0301	4.0026	0.8372	0.6740
Std. deviation	0.0404	0.8001	0.0156	1.5425	0.0076	0.0072

Table 4.7: Genetic algorithm optimization in "expanded" manipulation, ub_2 not fixed ($ub_2=x(4)$) – first left turn

N° trials	*K*	lb_2	a_2	ub_2	*RMSE_speed*	*RMSE_ax*
Trial 1	1.1223	1.1875	0.0198	4.0487	0.8310	0.6738
Trial 2	1.1070	0.3783	0.0154	3.5122	0.8307	0.6776
Trial 3	1.1042	0.1911	0.0149	3.6292	0.8307	0.6780
Trial 4	1.1147	2.9364	0.0125	5.8229	0.8312	0.6738
Trial 5	1.1677	0.1020	0.0551	4.5845	0.8550	0.6732
Mean	1.1232	0.9591	0.0235	4.3195	0.8357	0.6753
Std. deviation	0.0259	1.1857	0.0178	0.9397	0.0108	0.0023

Table 4.8: Genetic algorithm optimization in "narrow" manipulation, ub_2 fixed ($ub_2=lb_2+1$) – second left turn

N° trials	*K*	lb_2	A_2	ub_2	*RMSE_speed*	*RMSE_ax*
Trial 1	0.6178	0.5767	0.1975		0.7602	0.2686
Trial 2	0.9688	0.5580	0.0669		0.7405	0.2007
Trial 3	1.3663	0.1137	0.0078		0.7338	0.1779
Trial 4	1.3412	0.2492	0.0110		0.7338	0.1788
Trial 5	1.3145	0.6175	0.0009		0.7344	0.1784
Mean	1.1217	0.4230	0.0568		0.7405	0.2009
Std. deviation	0.3250	0.2267	0.0083		0.0113	0.0039

Table 4.9: Genetic algorithm optimization in "expanded" manipulation, ub_2 fixed ($ub_2=lb_2+1$) – second left turn

N° trials	*K*	lb_2	a_2	ub_2	*RMSE_speed*	*RMSE_ax*
Trial 1	1.3575	1.1867	0.0100		0.7338	0.1783
Trial 2	1.0953	1.4968	0.0500		0.7372	0.1918
Trial 3	1.2717	0.4402	0.0148		0.7340	0.1811
Trial 4	1.3131	0.3368	0.0127		0.7338	0.1797
Trial 5	1.1473	0.4980	0.0375		0.7357	0.1879
Mean	1.2370	0.3917	0.0250		0.7349	0.1838
Std. deviation	0.1114	0.1320	0.0178		0.0015	0.0058

Table 4.10: Genetic algorithm optimization in "narrow" manipulation, ub_2 not fixed ($ub_2=x(4)$) – second left turn

N° trials	*K*	lb_2	a_2	ub_2	*RMSE_speed*	*RMSE_ax*
Trial 1	1.0543	0.7574	0.0272	2.3272	0.7397	0.1887
Trial 2	0.9507	0.3086	0.0907	2.0226	0.7430	0.2025
Trial 3	1.1049	0.7310	0.0215	2.0020	0.7374	0.1865
Trial 4	0.8745	0.3817	0.1021	2.0059	0.7458	0.2094
Trial 5	1.0498	0.1125	0.0599	2.4714	0.7393	0.1907
Mean	1.0068	0.4582	0.0603	2.1658	0.7410	0.1956
Std. deviation	0.0927	0.2791	0.0363	0.2193	0.0033	0.0099

Table 4.11: Genetic algorithm optimization in "expanded" manipulation, ub_2 not fixed ($ub_2=x(4)$) – second left turn

N° trials	*K*	lb_2	a_2	ub_2	*RMSE_speed*	*RMSE_ax*
Trial 1	0.8817	0.0109	0.1019	3.0229	0.7472	0.2026
Trial 2	0.7760	0.1980	0.0915	3.7021	0.7559	0.2054
Trial 3	0.9350	0.1195	0.0714	3.0151	0.7444	0.1954
Trial 4	0.6272	0.4838	0.1361	3.0029	0.7643	0.2341
Trial 5	1.6974	0.0119	0.1418	3.7177	0.7603	0.2200
Mean	0.7835	0.1648	0.1085	3.2921	0.7544	0.2115
Std. deviation	0.1270	0.1949	0.0299	0.3815	0.0085	0.0155

From the Tables listed above, if we consider the mean value of each driver parameter for each combination, it is possible to notice that it is important not to keep ub_2 equal to $lb_2 + 1$, since in the cases where $ub_2=x(4)$, the difference between ub_2 and lb_2 oscillates from 1.71 (Table 4.10) to 3.37 (Table 4.6). Given such gap, it was supposed it was better to consider ub_2 as one of the driver parameters to be optimized through the genetic algorithm. Comparing the "expanded" and the "narrow" manipulation, instead, it was observed the difference between the mean values of each driver parameter was not so high; to increase the model generalization, the study proceeded by reducing more and more the gap between lower and upper boundaries, making the "narrow" manipulation even "narrower".

The parameters $\hat{a}_y$ and $\hat{a}_x$ need additional attention. These two parameters have no physical meaning once the driver gets close to the end of the turning stage: when this situation occurs, indeed, they both go to infinite. During the approach/turning stage, instead, anticipated accelerations represent an indication of the acceleration perceived by the driver. The anticipated accelerations are also useful in order to detect the crossover point, which is the point where the lateral acceleration becomes dominant with respect to the longitudinal acceleration. Before the crossover point the decision

to undertake the intersection (also called go/no go decision) must have been taken by the driver. By definition, this point is located before the turning stage starts: however, since the previous part of the results focused only on the turn stage, it has been necessary to take a closer look to the approach stage. Therefore, the time range has been extended in order to include also the final part of the approach stage and to identify the crossover point. Figure 4.6 shows the crossover point for the first left turn event. An oscillatory behaviour is presented by $\hat{a}_y$: an approximate evaluation of the change in heading angle $\Delta\varphi$, reliant on GPS data, is the main responsible of that. For $\Delta\varphi$ approaching values close to 29° (between $2.2 \cdot 10^5$ and $2.25 \cdot 10^5$ ms), $\hat{a}_y$ becomes lower with respect to $\hat{a}_x$. Once the crossover point for the first analysed left turn event was found, optimized driver parameters have been fixed to understand if the crossover point was really independent from them. Parameter values have been established by calculating the mean throughout Tables 4.6 - 4.7, the two tables which refer to the first left turn and consider ub_2 as a parameter to calculate through the genetic algorithm. Table 4.12 reports the optimized values of the parameters calculated by the genetic algorithm.

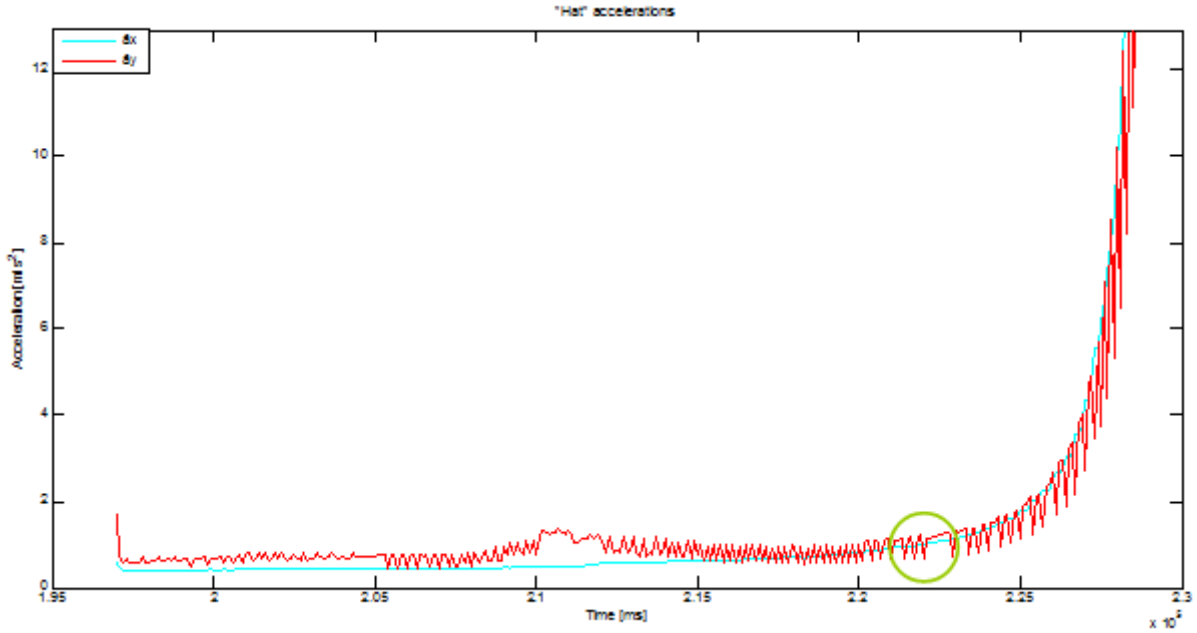

Figure 4.6: Crossover point for the first left turn

Table 4.12: Parameter values to find the crossover point (first left turn)

Parameter	K	lb_2	a_2	ub_2
Value	1.1284	0.7951	0.0268	4.1611

The same procedure has been performed for the second left turn event considered; also in this case the crossover point has been found for values of change in heading angle close to 29°. Result is shown in Figure 4.7. To conclude, the crossover points for other left turn events using the same parameter values collected in Table 4.12. The script was modified so that the upper and lower boundaries of the genetic algorithm coincided and were equal to the values in the above table. Results are shown in Figures 4.8 and 4.9. The oscillatory behaviour of $\hat{a}_y$ has been damped through the use of "*medfilt1*" function in MATLAB. As expected, even if the parameters were kept fixed, both the two anticipated accelerations tended to infinite as soon as the vehicle

reached the target point at the end of the turning stage. Anyway, if Figure 4.6 is compared to Figures 4.7 and 4.9, a main difference arises: in the former case, the lateral anticipated acceleration goes to infinite after the longitudinal one, as underlined by Nobukawa's work (which means, lateral acceleration grows in importance while turning with respect to longitudinal acceleration); in the latter cases, the opposite trend happens. The situation which occurs in Figures 4.7 and 4.9 should be further analysed, as it seems, in the two represented cases, that the driver pays more attention to the longitudinal than to the lateral acceleration. In Figure 4.8, instead, the same situation as in Figure 4.6 is present: the lateral acceleration, after an increasing trend, goes down to the level of the longitudinal one (crossover point) and then it rises again till it reaches infinite. Also in this case the oscillatory behaviour has been damped, but it was not possible, through the only use of the function "medfilt1" to dampen the steep oscillations present at the crossover point and at the end of the signal, when the vehicle was going to reach the target point.

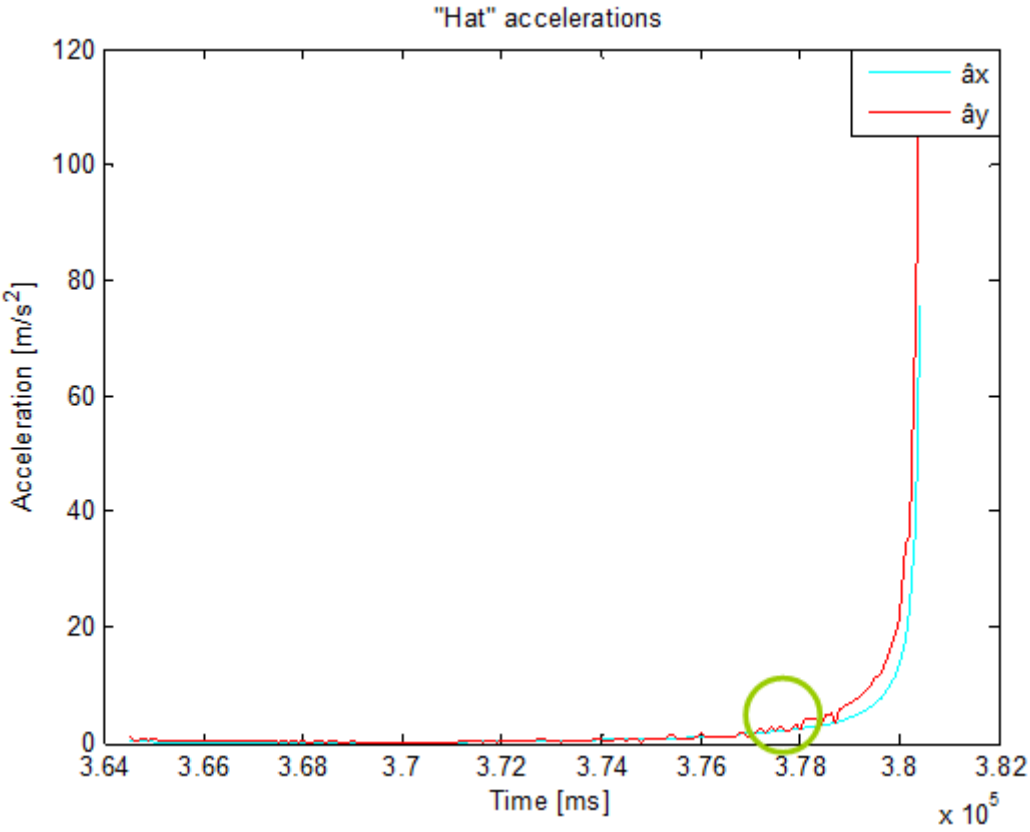

Figure 4.7: Crossover point for the second left turn event

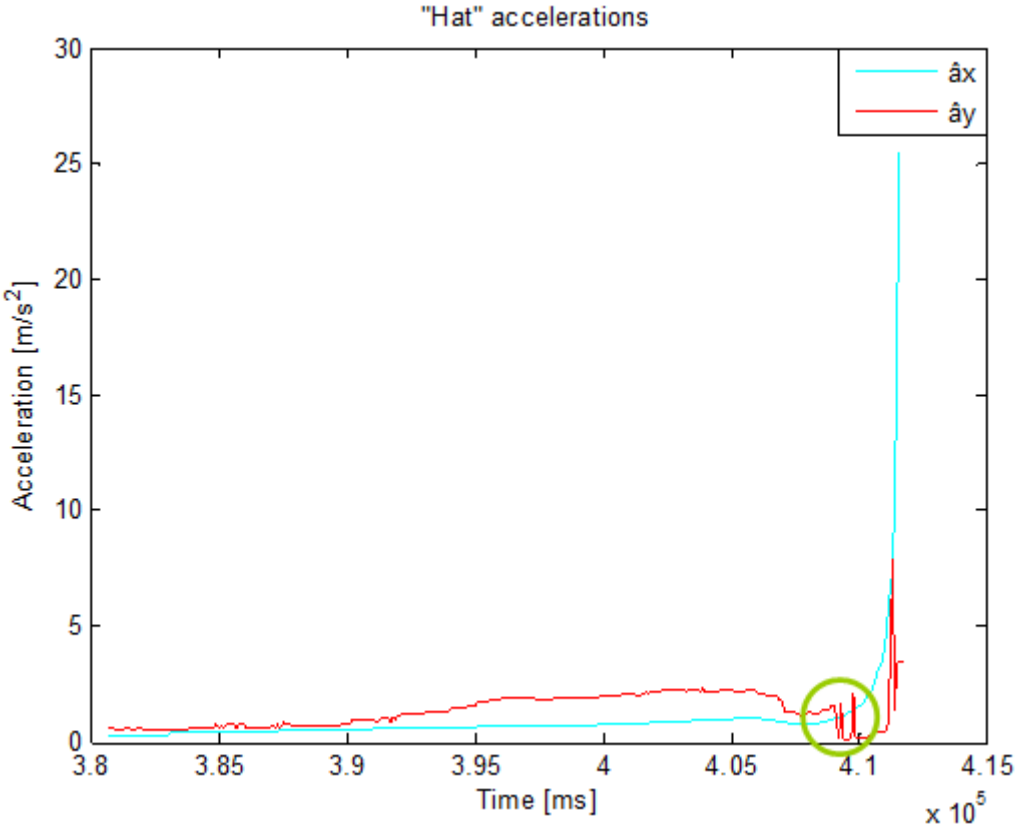

Figure 4.8: Crossover point for a third left turn event

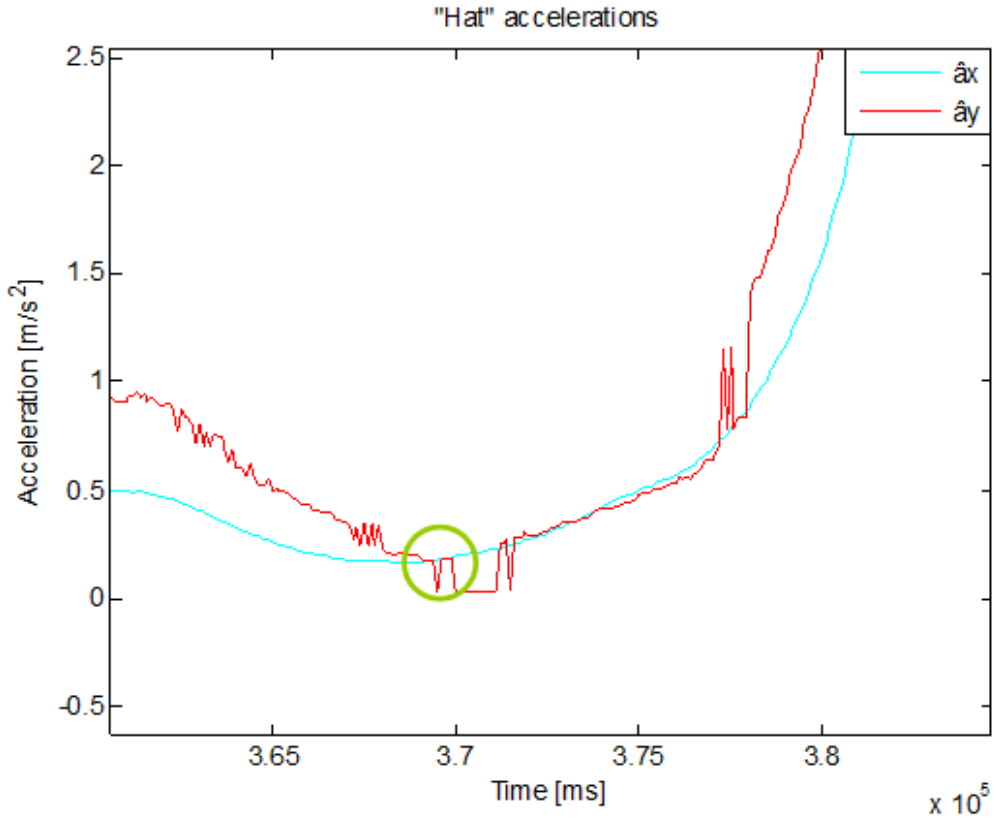

Figure 4.9: Crossover point for a fourth event

5 Discussion

5.1 Salvucci and Gray's model

The model presented in this thesis is an adaptation of the original model from Salvucci and Gray (2004), in which the authors utilize two different visual points (near and far points) that were also used in the driver behaviour model. However, compared to the Salvucci and Gray's model, the task performed by the driver is different since a left turn across path manoeuvre has being investigated. Given the specificity of the manoeuvre, the position of the near and far point proved to be critical for the scope of the work and a new definition was required, taking into account a shift of the coordinate system.

The model computed for a particular left turn intersection and for a specific driver show interesting results regarding the steering wheel angle rate and the steering wheel angle which models well the real data. The simulated trajectory of the vehicle shows a 90 degrees turn, in agreement with the real path travelled by the vehicle. The near and far point distances from the subject vehicle, during the left turn, were also reported. However, with regards to those variables, it is required a comparison with the values found in other intersections.

Looking at the results, the optimization procedure was successful for the left turn event considered but it is not possible to draw any conclusions about the generalization of the same optimization procedure to other intersection scenarios; changes in position of the near and far points and modifications to the script would be probably necessary to make the procedure suitable for other events.

With regards to the GA optimization employed for generating the seven parameters it was observed, after the analysis, that the parameter related to the cost function, named x(7), was not useful and could, therefore, be removed from the cost function. The parameters used to compute the steering wheel angle rate and that depend on driver characteristics (k_n, k_f, k_I) were, as well, generated by the GA. However, based on the work performed, it is not possible to know if the parameters describe well the driver under study and, also, if similar parameters could be employed to describe different drivers. In order to have a better understanding of the parameter values, a comparison was made with the values reported in Salvucci and Gray's paper. In the last one, in some cases, they reached values of, for example, k_I=36 which looks a bit far from the values the GA is generating in our case, in which values were normally in an interval of [-1;5] and hence the driver could not be really represented accurately by them. Nevertheless, the type of manoeuvre was different and it will be reasonable to have different values for the parameters even if the same driver performs both of them.

In further work, the parameters k_n, k_f, k_I would need to be included as an input of the model and not generated anymore by the GA. Also, it is relevant to mention that the upper and lower boundaries constraints of the parameters play an important role for the optimization; for example, if, despite the boundaries, the value of one parameter fluctuates around a constant number every time the model is executed the option of simplifying the model could also be possible; it could be replaced by this constant and the resulting model would then be simpler.

By adding the near and far point coefficients in the GA optimization, there is the intention of finding the best position of both of them being always the far point located further ahead than the near point. This arrangement differs from the approach

of Salvucci and Gray in which the near point remains at a fixed distance in front of the car and the far point changes depending on the road characteristics.

5.2 Nobukawa's model

The Nobukawa's model was used in this thesis to derive the speed profile during the intersection and, also, to find the crossover point that is relevant for the performance of the manoeuvre. Using the speed gathered from the real data, the speed profile model fits well the measured data in the intersections considered so far. Good results have been obtained also for intersections that are not "perfect" 90 degrees left turns, even if the intersections of this kind were very few; one of these examples is highlighted in Figure 4.7. When applying several times the genetic algorithm to the same intersection, the results show similar values for the parameters. However, if another intersection is considered, the parameters vary a bit, probably due to their dependence on the specific driver as already mentioned for the Salvucci and Gray's approach. Also, the results show that the parameter ub_2 cannot be kept fixed with respect to lb_2, as its value varies a lot when it is free to fluctuate as a parameter in the genetic algorithm.
For each iteration of the genetic algorithm, the values of the *RMSE_speed* and the *RMSE_ax* were calculated. As indicated by Nobukawa, these values should rarely be higher than 1 (10% probability), and that is what effectively happened even if it should be underlined that only two intersections were considered. The main limitation of the work is represented by the fact that the model adopts the speed obtained from the real data to estimate the speed. A relevant progress in the implementation of the model would be the utilization of the speed calculated at the time "t-1" for estimating the speed at time "t" instead of using the real data gathered from the Field Operational Test. This switch would mean passing from a static nature problem to a dynamic nature one.
The thesis also aimed to find the crossover point in the approach stage. Similar to the results found by Nobukawa, the crossover point is located few moments before $\hat{a}_x$ tends to go towards infinite, even if the values of $\hat{a}_y$ and $\hat{a}_x$ before the crossover point are quite different. Such difference, anyway, can be explained because Nobukawa's work and this thesis refer to different drivers and intersections. A limitation in the MATLAB® script arises if the same parameters are used to estimate the crossover point for different intersection events. Figures 4.9 and 4.11 are representative of such limitation: in these two cases, indeed, $\hat{a}_y$ tends to infinite before $\hat{a}_x$, while the opposite situation would be expected. This contradicts with what equations 2.29 and 2.30 state, since the change in heading angle should be decreasing as the vehicle is moving toward the exit stage. Further research is then needed in this sense, in order to understand if it is allowable to have $\hat{a}_y$ which tends to infinite before $\hat{a}_x$ or if the calculation of the change in heading angle must be performed using more detailed data than the available GPS ones.

6 Conclusions

Accident statistics show that intersections are a major cause of road fatalities because they require an accurate and timing decision making from the driver and, often, due to the presence of a Principal Other Vehicle (POV). Given that, this project focuses on intersections aiming to develop new models for the left-turn scenario. Considering the complexity of the topic, as a starting point, this thesis did not take into account the presence of the POV.

The work presented here tried to capture the main aspects of vehicle dynamics and driver behaviour in the attempt to merge, in the future, the two approaches in a unique model. To be able to do that, the thesis based its effort starting from two main theories, described in the "Literature review" section: Nobukawa, who deals with the speed and acceleration profiles of the vehicle, and relates them to driver reactions on the gas or brake pedal, and Salvucci and Gray, where precious information about perception based control theory for humans were extracted. In both models, the left-turn manoeuvre is described as divided in three stages, named respectively approach, turn and exit stage. At a first step, the work has only focused on the turning stage of the left turn event, in order to make analysis and code implementation simpler. Two models have been built based on the two theories above mentioned: they have been useful in modelling vehicle parameters such as the steering wheel angle rate, steering wheel angle, speed, vehicle trajectory and change in heading angle during the turning stage. Then, a deeper look to the other stages (especially the approach one) has been given, in order to identify the point, named crossover point, where the driver decides to either turn left or stop before performing the manoeuvre. It has been shown how to find such point and how to relate it to the target point located at the end of the turning stage, as described in Nobukawa's work. A brief analysis on the reliability of the two models has then been conducted.

The results reported in this thesis show that this work could be a first step towards the development of models to be used for future ADAS development. Of course, this work is characterised by some limitations; the main ones have been listed below:

- the models were applied to few intersections;
- few drivers have been considered;
- for Nobukawa model, the speed is obtained from the data and not from the model.

7 Future work

In the Nobukawa's model, the speed and acceleration profiles have been estimated in two different intersections investigated using as input the measured speed obtained from the data. The next step would be to make the system more independent, with the model providing the value of the speed at a certain time *t* basing on the longitudinal acceleration at the same time and the speed value at time *t-1*. The model should then count on the measured speed only for the initial value. A further step would be the testing of the model for different intersections and different drivers.

The driver behaviour model, derived from Salvucci and Gray, proved to work quite well in one specific left-turn event. The next step would consist in finding new left-turn events, performed by the same driver with the same turning angle as the one studied in order to check the model's validity and reliability. Then, a further step would require to check its validity also for different drivers and different trips. It is important to ensure that the model doesn't work only in a particular scenario and just describe a particular driver's behaviour but it should be reliable for all users performing a left turn across path with no POV. One risk with having several parameters describing a relatively simple event is that it may always be possible to find a reasonable fit.

The further work is not only focused on each model on its own. The merging of the two implemented models discussed in the thesis should be also performed. At the moment, it is not clear how this merging should be executed. One possibility would be representing by feeding the speed calculated by the Nobukawa's model into the Salvucci and Gray's model. However, other possibilities should also be taken into account.

After the merging of the two models, the final step would be the inclusion of the POV in the left-turn manoeuvre. This operation would affect both models as the driver would, in some cases, need to stop or change the speed and also adjust his/her decision making process to take account of the acceptance gaps.

An additional enhancement of the model would be represented by the inclusion of the approach stage and the exit stage during the left-turn.

8 References

Akamatsu M., Sakaguchi Y., Okuwa, M., 2003, "Modelling of driving behaviour when approaching an intersection based on measured behavioural data on an actual road", *in Proceedings of the Human Factors and Ergonomics Society 47th Annual Meeting.*

Allen B.L., Shin B.T., Cooper P.J., 1978, "Analysis of traffic conflicts and collisions", *Transportation research record* no.667.

Asano M., Alhajyaseen Wael K.M., Suzuki K., Nakamura H., 2010, "Modelling the variation in the trajectory of the left turning vehicles considering intersection geometry", *submitted for the presentation at the 90th Annual Meeting of the Transportation Research Board and publication in the Transportation Research Record.*

Bainbridge, L. , 1983, "Ironies of automation", *Automatica*, 19, 775-779.

Bekiaris, E., Petica, S., Brookhuis, K.A. 1997 "Driver needs and public acceptance regarding telematic in-vehicle emergency control aids", *in Proceedings of the 4th Word Congress on Intelligent Transport Systems. Brussel: Ertico*

Boda C.-N., Muñoz Cantillo J. C., 2013, "Field assessment of driver decision making at intersections", Master thesis.

Brookhuis K.A., de Waard D., Janssen W.H., 2001, "Behavioural impacts of Advanced Driver Assistance Systems – An overview", *Department of Psychology, University of Groningen.*

Brookhuis, K.A., Brown, I.D., 1992, "Ergonomics and road safety", *Impact of science on society*, 165, 35-40.

Cacciabue C. (Ed.), 2007, "Motivational Determinants of Control in the Driving Task" in: "Modelling Driver Behaviour in Automotive Environments Critical Issues in Driver Interactions with Intelligent Transport Systems", 165-188.

Cacciabue C. (Ed.), 2007, "Towards Understanding Motivational and Emotional Factors in Driver Behaviour: Comfort Through Satisficing" in: "Modelling Driver Behaviour in Automotive Environments Critical Issues in Driver Interactions with Intelligent Transport Systems", 189-207.

Cacciabue C. (Ed.), 2007, "Modelling Driver Behaviour on Basis of Emotions and Feelings: Intelligent Transport Systems and Behavioural Adaptations" in: "Modelling Driver Behaviour in Automotive Environments Critical Issues in Driver Interactions with Intelligent Transport Systems", 208-232.

Chan C.Y., 2006, "Characterization of driving behaviours based on field observation of intersection left-turn across path scenarios", *IEEE Transactions on intelligent transportation systems*, vol.7 no.3.

Chan, C.Y., 2005, "California intersection decision support: a systems approach to achieve nationally interoperable solutions."

Cody, D., Nowakowski, C., Bougler, B., 2011 "Observation of gap acceptance during intersection approach", *California PATH programme - Institute of Transportation Studies.*

Congress, 1994, "The Automated Highway System: an idea whose time has come", *Public Roads On-Line*, Summer 1994.

Damasio, A.R., 1994, "Descartes' error: Emotion, reason and the human brain", *G.P. Putnam's and Sons, New York.*

Dingus T.A., 2006, "The 100-Car Naturalistic Driving Study – Phase II – Results of the 100-Car Field", *National Highway Traffic Safety Administration*.

Donges, E., 1978, "A two-level model of driver steering behaviour", *Human Factors*, 20, 691–707.

ERSO, 2008, "Traffic safety basic facts 2008 – junctions, English", *available at: http://erso.swov.nl/safetynet/fixed/WP1/2008/BFS2008_SN-NTUA-1-3-Junctions.pdf*

Fildes B.N., Triggs T.J., 1985, "The effect of changes in curve geometry on magnitude estimates of road-like perspective curvature", *Perception & Psychophysics* 37 218 ^ 224.

FOT-Net, 2010, "Field Operational Tests – Evaluating ITS-applications in a real-world environment", *Seventh framework programme.*

Gillepsie T.D., 1992, "Fundamentals of vehicle dynamics", *Society of Automotive Engineers Inc.*

Hawkes A.G., 1968, "Gap-acceptance in road traffic", *Journal of applied probability*, vol. 5 no.1.

Holzman H., 2001, "Adaptive Kraftfahrzeugdynamik-Echtzeitsimulation mit Hybriden Modellen", *Forschritt-Berichte* VDI, Nr. 465.

Kessler C., Etemad A., Alessandretti G., Heinig K., Selpi S., Brouwer R., Cserpinszki A., Hagleitner W., Benmimoun M., 2012, "EuroFOT: bringing intelligent vehicles to the road – Final Report", *Seventh framework programme.*

Laberge J.C., Creaser J.I., Rakauskas M.E., Ward N.J., 2006, "Design of an intersection decision support (IDS) interface to reduce crashes at rural stop-controlled intersections", *Transportation research part C: emerging technologies*, vol. 14 no.1.

Land M F, Lee D.N., 1994, "Where we look when we steer", *Nature*, 369 742 ^ 744.

Land M, Horwood J, 1995, "Which parts of the road guide steering?" *Nature* 377 339 ^ 340.

Laureshyn A., 2006, "Assessment of traffic safety and efficiency with the help of automated video analysis."

Lee J., Lee J., Seung-Jin H., 2008, "Full vehicle dynamic modelling for chassis control", *School of Mechanics and Automotive Engineering, Kookmin University, South Korea.*

Levison W.H., Kantowitz B.H., Moyer M.J., and Robinson M., 1998, "A stopping-distance model for driver speed decision making in curve approach", *Proc. Hum. Factors Ergon. Soc. Annu. Meet*. 42, pp. 1222–1226.

Liebner, M., Klanner, F., Baumann, M., Ruhhammer, C., Stiller, C., 2013, "Velocity-Based Driver Intent Inference at Urban Intersections in the Presence of Preceding Vehicles", *in IEEE Intelligent Transportation Systems Magazine* 5, no. 2, p. 10–21

Naatanen, R. and Summala, H., 1974, "A model for the role of motivational factors in drivers' decision-making," Accident Analysis and Prevention, 6, 243-261.

National Highway Traffic Safety Administration, 2008, "National Motor Vehicle Crash Causation Survey-Report to Congress", *US Department of Transportation*.

National Highway Traffic Safety Administration, 2010, "Crash factors in intersection-related crashes: an on-scene perspective", *US Department of Transportation*.

National Highway Traffic Safety Administration, 2011, "Fatality Analysis Reporting System (FARS)", *US Department of Transportation*.

Nobukawa K., Gordon T.J., LeBlanc D.J., 2012, "Anticipatory speed control model applied to intersection left turns", *Vehicle system dynamics: International journal of vehicle mechanics and mobility.*

Pacejka H.B., Dixon J.C., 1991, "Lateral and longitudinal tyre forces", *ed. Springer*.
Preusser D.F., Williams A.F., Ferguson S.A., Ulmer R.G., Weinstein H.B., 1998, "Fatal crash risk for older drivers at intersections", *Accident analysis and prevention*, vol. 30 no. 2.
Ragland D.R., Arrojo S., Shladover S.E., Misener J.A., Chan C.Y., 2005, "Gap acceptance for vehicles turning left across on-coming traffic: implications for intersection decision support design", *TRB 2006 Annual Meeting*.
Rajamani R., 2012, "Vehicle dynamics and control," ed. Springer.
Rill G., 2003, "Vehicle dynamics", *Lecture notes, Hochschule für Technik Wirtschaft Soziales.*
Rosengren, L.G., 1995, "Driver assistance and co-operative driving", in *ERTICO (Ed.), Towards an intelligent transport system. Proceedings of the First World Congress on Advanced Transport Telematics and Intelligent Vehicle Highway Systems.* London: Artech House, 1613-1622.
Rumar, K. 1988, "Collective risk, but individual safety", *Ergonomics*, 31: 507-518.
S. Aoude, V. R. Desaraju, L. H. Stephens, and J. P. How (2011), "Behavior Classification Algorithms at Intersections and Validation using Naturalistic Data", *in IEEE Intelligent Vehicles Symposium*, pp. 601–606.
Salvucci, D. D., 2006, "Modelling driver behaviour in a cognitive architecture", *Human Factors*, 48, 362 – 380.
Salvucci, D., & Gray, R., 2004, "A two-point visual control model of steering", *Perception*, 33, 1233–1248.
Summala, H., 1988, "Risk control is not risk adjustment: The zero-risk theory of driver behaviour and its implications", *Ergonomics*, 31,491-506.
Taylor, D.H., 1964, "Drivers' galvanic skin response and the risk of accident", *Ergonomics*, 7,253-262.
Treat J.R., Tumbas N.S., McDonald S.T., Shinar D., Hume R.D., 1979, "Tri-level study of the causes of traffic accidents – An executive summary", *National Technical Information Service*.
Vaa, T., 2001, "Driver behaviour models and monitoring of risk: Damasio and the role of emotions." Proceedings from VTI-Conference Traffic Safety on Three Continents. Moscow 19-21 September 2001.
Verwey, W.B., Brookhuis, K.A., Janssen, W.H., 1996, "Safety effects of in-vehicle information systems", *Soesterberg, the Netherlands: TNO Human Factors Research Institute.* Report TM-96-C002.
Wang, J., 2004, "Friction estimation on highway vehicles using longitudinal measurements", *ASME Journal of dynamic systems, measurement and control.*
Weinheim C. H., 2001, "Adaptive semiphysikalische Echtzeitsimulation der Kraftfahrzeugdynamik im bewegten Fahrzueg", *Forschritt-Berichte* VDI, Nr. 467.
White R.A., Korst, 1972, "The determination of vehicle drag contributions from coast-down tests", *Society of Automotive Engineers Inc.*
Wilde, G.J.S., 1982, "The theory of risk homeostasis: Implications for safety and health Risk Analysis", 2, 209-225.

9 Appendices

9.1 Appendix A: Division of work

Patrick Bardinet de Horna:

- Literature review
- EuroFOT data analysis and extraction
- Matlab functions Research and study: Genetic Algorithm
- Salvucci and Gray driver model analysis and implementation.
    - New scenario
    - Definition of near and far points
- Previous model code analysis
    - Validity of code in new conditions
    - Adaptation for left turn scenario
- Coding:
    - Matlab programming
    - Genetic algorithm parameters and options decision
    - Code debugging
- Analysis of results
- Report writing

Francesco Secondo:

- Literature review
- EuroFOT data analysis and extraction
- Matlab functions Research and study: Genetic Algorithm
- Nobukawa et al. vehicle model analysis
    - Simulation program coding and adaptation to left turn scenario
    - Code validation
    - Definition of vehicle speed and acceleration profiles
    - Definition of crossover point
- Coding:
    - Matlab programming
    - Genetic algorithm parameters and options decision
    - Code debugging
- Analysis of results
- Report writing